Review Article

Kun Yuan#, Danting Shu#, Xing Li, Zihao Guo, Xiang Ren, Yiqun Tian, Zhenliang Qin, Zhixian Wang, Jing Wang, Yisheng Yin, and Xiaoyong Zeng*

Micro/nanomotors in biomedicine: Construction and applications

https://doi.org/10.1515/ntrev-2025-0176
received July 4, 2024; accepted May 12, 2025

Abstract: The significant potential for autonomous movement and adaptable modification has made micro/nanomotors (MNMs) a major focus of research and application in biomedicine. However, current designs for MNMs face several unresolved issues, including improving propulsion methods, precise navigation control, expanding application ranges, ensuring biological safety, and achieving multifunctionality. This review provides a comprehensive overview of recent progress in the application of MNMs in biomedicine, focusing on propulsion mechanisms, targeting strategies, structural design, and practical applications. We also analyze the connections between these aspects and propose future directions for developing multifunctional platforms with various propulsion methods. The goal of this review is to promote the translation of nanorobotic technologies into clinical practice and establish a foundation for their ongoing development.

Keywords: micromotors, nanomotors, biomedical applications, propulsion mechanisms, tumor therapy

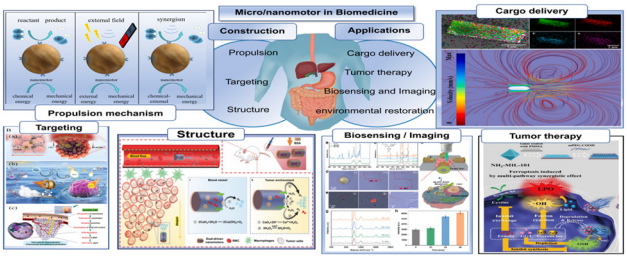

Graphical abstract

1 Introduction

In recent decades, significant progress has been made in the development of passive delivery systems using nanoparticles (NPs), in both laboratory and clinical settings. However, the effectiveness of these NPs in biomedical applications relies on their ability to navigate and overcome complex biological barriers, dense extracellular matrices, and challenging biofluids through self-diffusion processes [1]. The delivery of cargo faces numerous obstacles in practical applications due to the complex microenvironment of the human body. Passive delivery strategies alone are insufficient for achieving optimal task execution, revealing the limitations of non-designed nanoscale structures in meeting the ever-evolving requirements of medical applications. The comparative analysis between micro/nanomotor (MNM)-based delivery technology and other delivery systems is summarized in Table 1.

Inspired by natural molecular motors [8], researchers have explored the construction of artificial microscale self-propulsion systems. Ismagilov *et al.* developed a system, serving as a precursor to microscale motors, that autonomously propels itself by consuming fuel from its environment. Under experimental conditions, the system demonstrated approximate stability over a 2 h period, sustaining motion for several days and restoring motion to initial levels through replenishing hydrogen peroxide (H_2O_2) [9]. Paxton *et al.* fabricated Au/Pt bimetallic nanorods that catalyze the decomposition of H_2O_2, leading to bubble formation. These nanorods exploit variations in solution surface tension gradients and electric fields generated by proton transfer in redox reactions

# These authors contributed equally to this work and should be considered first co-authors.

* **Corresponding author: Xiaoyong Zeng**, Department of Urology, Tongji Hospital, Tongji Medical College, Huazhong University of Science and Technology, No.1095 Jiefang Avenue, Wuhan, 430030, Hubei, China, e-mail: miwai@163.com, tel: +86-027-69378205
Kun Yuan, Xing Li, Zihao Guo, Xiang Ren, Yiqun Tian, Zhenliang Qin, Zhixian Wang, Jing Wang, Yisheng Yin: Department of Urology, Tongji Hospital, Tongji Medical College, Huazhong University of Science and Technology, No.1095 Jiefang Avenue, Wuhan, 430030, Hubei, China
Danting Shu: Institute of Life Science, and Laboratory of Tissue and Cell Biology, Lab Teaching & Management Center, Chongqing Medical University, Chongqing, 400016, China

Table 1: Comparison between delivery based on MNM-based and other delivery methods

Delivery method	Description	Advantages and applications	Disadvantages	Ref.
Delivery based on MNMs	A novel nanodelivery technology that relies on asymmetric structures can convert ambient energy into self-propelling mechanical energy	Unique active mobility and excellent targeting ability Powerful to modifiability meet diverse needs A wide range of applications	The production and preparation costs are high The biocompatibility depends on the preparation technology The stability is poor, and storage is challenging	[2]
Liposomes	Ordered bilayer lipids form closed vesicles with hydrophobic shells and hydrophilic nuclei	Liposomes have a unique structure and good biocompatibility for normal metabolism. They are often used to reduce drug toxicity and avoid its accumulation in the body. They have unique advantages in assisting the load to cross biological barriers	Low loading capacity High production cost Instability Poor targeting ability	[3]
Metal and inorganic NPs	Artificially selected NPs of various delivery materials	High specific surface area Rich variety Low preparation cost Strong modifiability Wide range of applications	Their biocompatibility needs improvement, and the mechanisms of toxicity, metabolism, and clearance *in vivo* are not yet clear	[4]
Cell membrane	A carrier prepared by preserving the cell membrane structure	Excellent biocompatibility Non-immunogenic Cell membrane proteins provide targeting Cell membrane carriers are effective at carrying substances that need to prolong blood circulation time	Poor stability Difficult to store Narrow application scope	[5]
Exosomes	Extracellular vesicles are vesicles secreted by most cells, with an average diameter between 40 and 100 nm, containing DNA RNA, proteins, and other substances	Extracellular vesicles themselves have some unique biomedical functions such as promoting or inhibiting cell growth, low preparation cost, certain targeting, and good biocompatibility	The preparation steps are cumbersome Poor stability Insufficient research on biological effects	[6]
Hydrogel	Hydrogel is a network structure cross-linked by physical or chemical methods, which can expand in an aqueous environment	Excellent biocompatibility and biodegradability, low cost Hydrogels are often used for drug sustained release	In practical application, hydrogels have poor controllability, a limited scope of action and cannot provide targeting	[7]

to propel themselves axially in H_2O_2-rich environments. The insights gained from understanding their propulsion mechanism have contributed to advancements in MNM technology [10,11].

The functionality of a system is determined by its construction. In the process of constructing MNMs, three fundamental elements are involved: propulsion, targeting, and structure. Researchers have engineered nanostructures capable of effectively converting various fuels, such as H_2O_2 [12–15], water [16], glucose [15,17,18], and urea [19–23], through redox reactions or energy from external stimuli, such as ultrasound (US) [24–29], light [30–39], electricity [40], and magnetism [41–45], into mechanical energy for propulsion. These designed nanostructures exhibit the ability to actively navigate complex environments and perform biomedical tasks as intended.

Throughout the developmental trajectory, chemotaxis induced by gradients in substance concentrations within the working environment [46] has been the earliest and most widely employed targeting modality. Its advantages lie in its stability and generalizability. However, the increasing demand for targeting precision and complexity in working environments necessitates more advanced designs. Various parameters of external physical fields offer unique adjustability, enabling targeted navigation by MNMs through parameter modulation [47,48]. Subsequently, the specificity and affinity of receptor–ligand interactions in biological organisms have been recognized, yielding satisfactory outcomes [49]. Currently, researchers have endeavored to achieve targeting at the single-cell, subcellular, and molecular levels through a series of complex biological reactions and artificial interventions [50].

An asymmetric structure is commonly referred to as a Janus nanostructure and is characterized by an asymmetrical configuration with distinct physical or chemical properties on opposite sides [51]. MNMs with Janus structures are currently the most extensively researched category of MNMs. In these MNMs, scientists achieve propulsion by deliberately modifying the driving components on the substrate unevenly, allowing a portion of the MNMs to function as an engine that propels overall movement. The defining feature of these MNMs lies in their ability to autonomously disrupt static equilibrium, relying on their inherent asymmetry to exhibit directed, active motion [52]. On the other hand, specific nanocatalysts designed based on Janus structures demonstrate higher catalytic activity than their pure particle counterparts, potentially offering enhanced propulsion capabilities in the design of MNMs [53]. MNMs have been utilized as multifunctional carriers in complex biomedical tasks, including drug delivery [54–61], disease therapy [62–75], diagnosis, biosensing [76–89], and environmental restoration [89–92]. Precision medical technologies based on MNMs possess minimally invasive operation, targeting, intelligence, and broad applicability, providing distinct advantages over traditional medical techniques.

However, MNMs currently face various challenges, including biosafety, propulsion, structure, navigation, and *in vivo* safety. Previous studies have often focused on application development while neglecting the connection between structure and function. Nonetheless, it is important to recognize that the construction of systems and their applications have a mutually influential relationship. Therefore, this review emphasizes the relationship between the building elements of MNMs and their applications. The choice of propulsion, components for structural loading, and targeting processes all significantly impact the efficiency of biomedical tasks.

This review begins by providing an overview of the three major elements of MNM construction: propulsion, targeting, and structure. We point the current issues associated with these elements and examine the attempted solutions. Our discourse also analyzes the current status and summarizes the development trends in various fields to provide researchers with valuable insights. Additionally, this review outlines the primary applications of MNMs in the biomedical field, discusses the development trends, and establishes directions for the advancement of multimode propulsion and multifunctional integration platforms.

2 Construction and classification

In this section, we discuss the three essential elements involved in the construction of MNMs: propulsion mechanisms, targeting modalities, and structural components. Propulsion mechanisms provide MNMs with the ability to move autonomously, while targeting modalities determine the efficiency of task execution. Extensive research has been conducted to advance MNMs in these areas, resulting in improved locomotion capabilities characterized by increased speed and controllability. Achievements include precise targeting at the single-cell and subcellular levels. A significant recent advancement in the field of MNMs is the integration of biological components, known as biohybrid structures, to enhance performance. Existing studies have demonstrated the unique potential of these structures for various applications. However, further in-depth research is necessary to advance our understanding of emerging paradigms.

2.1 Propulsion

The movement of microscale objects is primarily influenced by viscous forces. At the nanometer level, the effect

of inertia becomes negligible [93]. Therefore, continuous motion requires sustained, stable power to overcome the static equilibrium caused by viscous forces [52]. Interactions between MNMs and solvent molecules include Brownian motion collisions, chemical reactions, and physical shape changes [10]. The speed and size of MNMs are critical quantitative parameters that directly influence their performance in biomedical applications. Speed allows MNMs to navigate through bodily fluids (such as blood, urine, and cerebrospinal fluid), improving overall operational efficiency. Size impacts both targeting and stability; specifically, particles smaller than 5 nm are more likely to be cleared by the immune system, while those larger than 500 nm tend to accumulate in the liver [94]. This places high demands on the stability of power components. To meet these requirements, various driving methods have been developed to provide energy for MNMs. The future development of propulsion methods for MNMs lies in flexible selection of driving methods based on specific needs and personalized design and combination.

MNMs can be classified into three categories based on the different ways they obtain power: redox reaction driven, external field driven, and synergistic driven (Figure 1).

2.1.1 Redox reaction driven

Redox reaction-driven MNMs derive energy from solutes through redox reactions to propel their motion. This reaction requires MNMs to catalyze the decomposition of molecules within solutes or to react with substances in solutes to generate concentration gradients or bubbles for axial movement. Sen *et al.* pioneered the development of redox reaction-driven MNMs for the transportation of polystyrene (PS) particles [95]. The primary mechanisms for redox reaction-driven propulsion include bubble propulsion, self-diffusiophoresis, and self-electrophoresis. Enzymes, highly efficient biological catalytic components, have been extensively used in the construction of these propulsion mechanisms. Recently published redox reaction-driven MNMs and their size, motion speed, propulsion mechanisms, power components, and applications are summarized in Table 2.

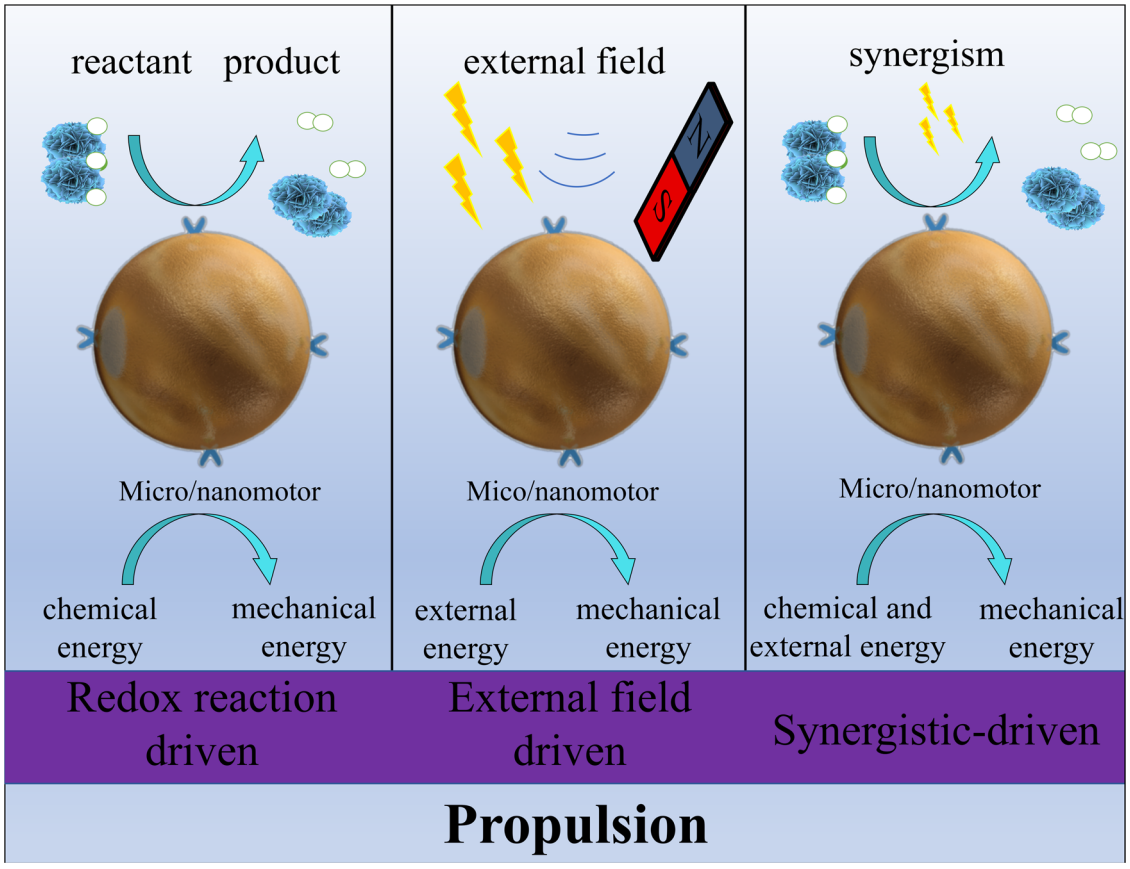

Figure 1: Propulsion mechanisms of nanomotors: redox reaction driven (left), external field driven (middle), and synergistic driven (right).

Table 2: Comparative analysis of MNMs and their application in biomedicine (redox reaction driven)

MNMs	Size	Motion speed	Propulsion mechanism	Power components	Applications	Ref.
Au@MSN/CORM-401@HA	82 nm	4.24 μm/s	Bubble propulsion (CO)	CORM-401	Treatment renal injury	[96]
MIL-GOx-ALA	293 ± 3 nm	4.8 μm/s		5-ALA	Treatment tumor	[97]
Au@SS31-TK-MSN/GYY4137@S	73 nm	4.62 μm/s	Bubble propulsion (H_2S)	Prodrug GYY4137	Treatment renal injury	[98]
PEG-Cys@PEG	100 nm	3.5 μm/s		L-cysteine	Treatment Parkinson's disease	[99]
NM@hydrogel	60.0 ± 5.0 nm	10.1 ± 1.1 μm/s	Bubble propulsion (CO_2)	$CaCO_3$	Treatment tumor	[100]
Pt@HSNs(DQ)	290 nm	3.25 ± 0.66 μm/s	Bubble propulsion (O_2)	Pt	Treatment tumor	[12]
MOS/Pt	192.2 ± 1.1 nm	8.53 μm/s		Pt	Treatment suppurative otitis media	[13]
Pt-Pd-Mo-JCN	106 nm	—		Pt-Pd-Mo	Treatment Emergency Rescue of Traumatic Brain Injury	[14]
CAT-ZIF-8	—	—		H_2O_2-decomposing enzyme catalase (CAT)	pollutant removal	[101]
GC6@cPt ZIFs	70–120 nm	2.08 μm/s		Pt	Treatment tumor	[15]
Pt/DOX/LOX/LM cRGD	110 nm	—		Pt	Treatment tumor	[64]
/	241 ± 25.9 nm	—		Glucose oxidase and CAT	Pollutant removal	[102]
Pt/Pd-FeCNCs	L ~ 915 ± 58 nm W ~ 53 ± 9 nm	1–10 μm/s		Pt	Treatment thrombolysis	[103]
LDH nanosheet-based NMN	100 nm	2.09 μm/s		LDH-nanosheet	Treatment tumor	[104]
Mg@anti-CD3	20 ± 5 μm	50 ± 24 μm/s	Bubble propulsion (H_2)	Mg	Treatment tumor	[16]
AG-DMSNs	80 nm	10.9 μm/s	Bubble propulsion (NO)	L-arginine	Treatment Antibacterial	[105]
MS/LA/RGD/UK	200 nm	3.52 μm/s			Treatment thrombolysis	[106]
HFCA/DTX/aPD1	40 nm	—			Treatment tumor	[107]
Dielectric-AgCl	—	—	Self-diffusiophoresis	AgCl	—	[108]
As-Pt/DOX	202 nm	8.1 μm/s		Pt	Cargo delivery	[109]
SiO_2($mSiO_2$)/SiO_2/Au with ureases	2.31 ± 0.26 μm	18 μm/s		Ureases	—	[22]
PEG-modified Janus AuNP	30–100 nm	—			—	[20]
–.	418 ± 21 nm	1.47 ± 0.04 $\mu m^2/s$			Cargo delivery	[21]
Pdop@enzyme@aZIF-8	200 nm	8.3 $\mu m^2/s$			Treatment tumor	[23]
Cu-Pt nanorods	3.6 μm	7 μm/s	Self-electrophoresis	Cu-Pt	—	[110]

"–" means no given data in the references.

HA: hyaluronic acid; ALA: aminolevulinic acid; TK-SS31 D-Arg-dimethylTyr-Lys-PheGYY4137 NH_2: (methoxyphenyl)(morpholino) phosphorodithioic acid; NM: nanomotor; HSNs: hollow silica nanomotors; MOS: mesoporous organosilica; CAT: H_2O_2-decomposing enzyme catalase; GC6: glucose oxidase (GOx); CAT: catalase; Ce6: chlorin e6, CNCs: cellulose nanocrystals; LDH: layered double hydroxide, AG-DMSNs: L-arginine (L-Arg) and gold nanoparticle (AuNP)-loaded dendritic mesoporous silica nanoparticles; MS: mesoporous silica; LA: L-arginine; RGD: arginine–glycine–aspartic acid; UK: urokinase; HFCA: heparin–folate–cy5.5/L–arginine; DTX: docetaxel; Pdop: polydopamine; $\mu m^2/s$: diffusion coefficient.

2.1.1.1 Bubble propulsion

Bubble propulsion is a widely studied and well-established method of propulsion in the field. MNMs, which can function as catalysts or fuel carriers, induce motion by utilizing the continuous momentum change caused by bubbles detaching from them. The most common fuel used in this context is H_2O_2 [111]. In addition to catalyzing the production of oxygen for propulsion, there is growing interest in exploring the synergistic effects of various gas molecules in disease treatment processes. For example, O_2 [12], nitric oxide (NO) [105–107], carbon monoxide (CO) [96,97], hydrogen sulfide (H_2S) [98,99,112], H_2 [16,113], and CO_2 [100] have all become research hotspots due to their potential therapeutic effects. It becomes evident that this process significantly impacts the composition of the microenvironment, as certain substances in the microenvironment are consumed. Therefore, investigating these effects has become an important area of research.

Bubble propulsion not only provides power for MNMs but also offers therapeutic benefits for disease alleviation. Studies have reported that H_2O_2 decomposition, catalyzed by Pt in drug-loaded MNMs, generates oxygen bubbles that not only propel the motors but also enhance the effectiveness of chemotherapy by overcoming multidrug resistance (Figure 2a) [12]. However, the toxic effects of H_2O_2 on organisms limit the motion of single-metal MNMs propelled by this compound at physiological concentrations. Recent studies have proposed a novel therapeutic approach by combining Janus mesoporous organosilica /Pt MNMs with H_2O_2 cleansing agents. The active motion of these motors facilitates the accumulation of antibiotics [13]. To enhance the locomotion capabilities of MNMs at low concentrations of H_2O_2, another solution involves improving the composition of their catalytic components. This can be achieved by forming Pt–Pd alloys doped with active Mo atoms, which have been shown to exhibit higher rates of H_2O_2 adsorption and catalytic efficiency than traditional Pt catalysts [14]. Water, one of the decomposition products of H_2O_2, is widely present in biological organisms and can be used as a fuel source for MNMs. The biocompatibility of

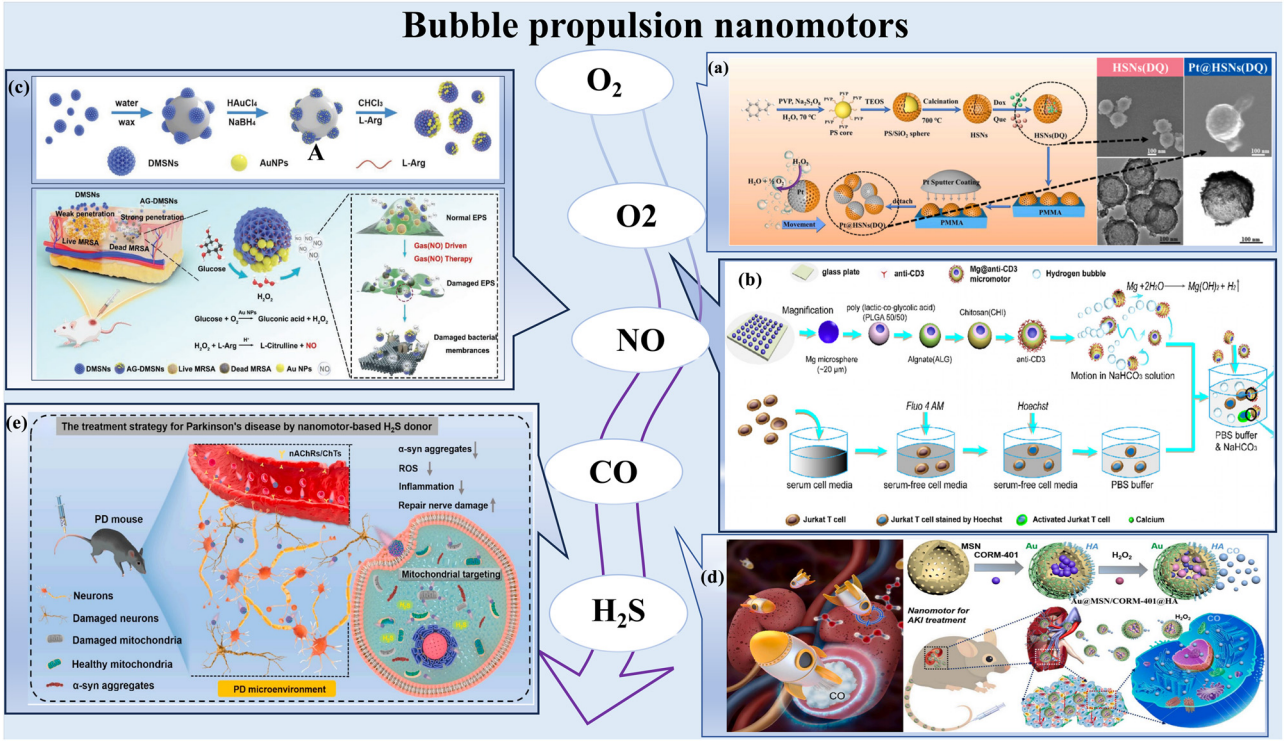

Figure 2: Bubble propulsion nanomotors: (a) synthetic procedure (left) and SEM images (right) for the preparation of Pt@HSN from the study by Zhou *et al.* [12], (b) scheme of the fabrication of the Mg@anti-CD3 MNMs from the study by Chang *et al.* [16]; (c) schematic diagram illustrating the synthesis (top) and penetration (bottom) of methicillin-resistant *Staphylococcus aureus* biofilms by AG-DMSNs from the study by Zheng *et al.* [105]; (d) schematic diagram depicting the therapeutic application of CO-driven AMCH for treating AKI (right) and its movement *in vivo* and *ex vivo* (left) from the study by Tong *et al.* [96]; and (e) schematic diagram illustrating the treatment of Parkinson's disease (PD) using H_2S-driven PCM from the study by Zhao *et al.* [99]. SEM: scanning electron microscope; HSN: hollow silica nanocapsule; AG-DMSNs: nanomotors based on L-arginine and gold nanoparticle-loaded dendritic mesoporous silica nanoparticles; AMCH Au@MSN/CORM-401@HA: AKI: acute kidney injury; PCM: polyethylene glycol modified with L-cysteine nanomotors and 2-methacryloyloxyethyl phosphorylcholine.

water also offers advantages in fuel selection, with magnesium (Mg) being a cost-effective construction component commonly used. Wang *et al.* developed a Mg MNM system loaded with anti-CD3, which has degradable components and reacts with H_2O to promote hydrogen propulsion (Figure 2b) [16,114]. The system can reach a movement speed of 50 ± 24 μm/s, which is ahead of other bubble-propelled MNMs.

A recent research trend involves utilizing gas molecules to propel MNMs for active motion and to leverage their associated functions during task execution. Upon release into the microenvironment, gas molecules can remodel the disease-specific internal environment, participate in biochemical reactions, influence disease progression, facilitate *in vivo* imaging, and assist in therapy. For instance, NO serves as a crucial signaling molecule in the human body and plays a significant role in cascading pathophysiological reactions. The antimicrobial nanomotors designed by Zheng *et al.* can catalyze the decomposition of glucose to produce H_2O_2, which subsequently oxidizes L-arginine (L-Arg) to generate NO for propulsion (Figure 2c) [105]. Tao *et al.* reported a gas bubble-propelled drug delivery system that achieved high drug retention. They modified bowl-shaped mesoporous silica nanoparticles (MSNs) with arginine–glycine–aspartic acid (RGD) peptide to confer thrombus-targeting capability to the drug carrier system, resulting in the synthesis of MS/LA/RGD/UK MNMs. In this system, NO not only acted as a driving force to enhance MNM penetration and drug utilization efficiency but also stimulated endothelial cell growth for vascular repair [106]. Research has demonstrated the synergistic therapeutic effect of chemotherapy/immunotherapy through the interaction between drugs and NO during the immune response process [107].

Another example is a CO-propelled MNM designed for the treatment of acute kidney injury (AKI). It comprises amine-functionalized MSNs (NH_2-MSNs) as the substrate and is modified with cORM-401. One side is tailored with hyaluronic acid (HA) for renal tubule targeting, while the other side is decorated with gold nanoparticles (AuNPs). Within the microenvironment of AKI, H_2O_2 reacts with cORM-401, releasing the therapeutic factor CO (Figure 2d) [96]. CO can disrupt mitochondrial function, inducing apoptosis in tumor cells. The asymmetric Janus structure represented in this study is currently one of the most extensively researched types of MNMs. In practical applications, these MNMs can move at high speeds and quickly reach targeted locations. However, the purely asymmetric structure is prone to damage, which can lead to a loss of functionality, making it unsuitable for storage and operation in complex environments. Selective release is crucial due to its toxic effects in the bloodstream. Chen *et al.* employed a cascade reaction-based design using 5-aminolevulinic acid as the CO donor. Upon delivery by MNMs to the lesion site, the enzyme undergoes condensation reactions to synthesize heme, which is subsequently catalyzed by heme oxygenase-1, which is overexpressed in tumor cells, leading to CO generation [97]. This strategy has successfully achieved selective and responsive release by reducing CO leakage.

Following NO and CO, H_2S is recognized as the third gasotransmitter in the human body. There is increasing evidence suggesting its therapeutic and preventive effects on various diseases. Consequently, researchers have naturally incorporated H_2S into the design of MNMs for active locomotion systems [112]. Treatment of AKI with H_2S involves the release of low levels of H_2S *via* MNMs delivery of (methoxyphenyl)(morpholino)phosphorodithioic acid (GYY4137), along with selective binding to cardiolipin of the mitochondrion-targeted antioxidant D-Arg-dimethylTyr-Lys-PheNH2 (TK-SS31), thereby protecting mitochondrial cristae from AKI-induced damage [98]. A decrease in endogenous H_2S levels is also implicated in the progression of PD. One study demonstrated the differential catalytic abilities of mitochondrial 3-mercaptopyruvate sulfurtransferase (3-MST) and cystathionin β-synthase (CBS) in neurons at PD sites in the brain, which provided chemotaxis ability to the delivery system. This is attributed to the specific expression of 3-MST within mitochondria and its superior ability compared to that of CBS to catalyze the production of H_2S in the blood. This not only fulfills the objective of ameliorating the PD microenvironment but also mitigates unnecessary H_2S release into the bloodstream (Figure 2e) [99].

In summary, bubble propulsion is the most widely studied and mature propulsion methods, offering advantages such as autonomous energy supply without external energy support. In disease treatment, bubble propulsion can also reshape the disease microenvironment by releasing gas molecules and affect the disease process. Although its propulsion speed is relatively high, this method struggles to achieve continuous propulsion and accurate direction.

2.1.1.2 Self-diffusiophoresis and self-electrophoresis

Self-diffusiophoresis is another predominant propulsion mechanism for MNM locomotion, wherein concentration gradients or ion charge gradients propel the motion of nanomachines. The distinction between non-ionic diffusion electrophoresis and ion diffusion electrophoresis is that the substances used to establish concentration gradients are electrically neutral.

Zhou *et al.* conducted a study on the mechanism of ionic self-diffusiophoresis, focusing on ion-driven self-diffusiophoresis achieved through the use of a photochemically driven AgCl Janus MNMs. Researchers utilized $FeCl_3$ to reduce Ag-coated poly(methyl methacrylate)-based Janus spheres into AgCl, which was then decomposed into Ag through exposure to visible light. The resulting H^+ ions diffused faster than the Cl^- ions, resulting in a low electric potential near the AgCl surface, initiating the motion of charged colloidal particles [108]. However, the high ion concentration within the system limits the locomotion functionality of self-electrophoresis-driven MNMs. To address this issue, Yang *et al.* developed miniature MNMs, ranging in size from 100 to 30 nm, with AuNPs as the core and urease as the propeller (UPJNMs). These UPJNMs overcome motility loss in high ion concentration environments, a challenge faced by other self-electrophoresis MNMs due to ion quenching [20]. Another study by Rosli *et al.* involved the modification of arsenene NPs with platinum to form Janus As-Pt MNMs (size: 202 nm, motion speed: 8.1 μm/s), which exhibited bubble-free diffusiophoresis [109].

Self-electrophoresis occurs when oxidation and reduction reactions occur at the anode and cathode of MNMs, leading to an uneven distribution of ions near the carrier. This asymmetry generates a local electric field, resulting in electrophoretic effects that propel the motion of charged MNMs [115]. In the case of Cu-Pt nanorods designed by Liu and Sen, bubble-free self-electrophoretic propulsion was observed when the MNMs were placed in Br_2 or I_2 solutions, with the copper end serving as the anode. According to the Galilean inverse principle, the system is expected to move toward the copper end, which aligns with the observed behavior. Experimental validation also revealed that the rod's velocity scales proportionally to the current density and the concentration of Br_2/I_2 but is inversely proportional to the rod's length. This study highlights the wide applicability of self-electrophoretic propulsion in MNMs [110].

It is important to note that both self-diffusiophoresis and self-electrophoresis are still in research stages, and many related mechanisms have yet to be fully understood. Existing theories are unable to explain all phenomena, providing an opportunity for further advancements in MNMs through improved interpretations of these processes [116,117].

2.1.1.3 Enzyme-driven

Enzymes have been extensively utilized and developed in the aforementioned three categories of MNMs. Therefore, it is necessary to discuss enzymes separately in this context. The use of enzyme catalysis, compared to non-enzyme materials as driving components, offers several advantages for designing chemically powered MNMs. These advantages include a longer lifetime, as well as unique features such as biocompatibility, versatility, and bioavailability of fuel [118,119]. Furthermore, the specific affinity between enzymes and substrates can be leveraged for targeting purposes.

The selection of enzymes and substrates plays a crucial role in these research, directly influencing the structure of MNMs and the efficiency of task execution. Glucose, a commonly found energy-supplying molecule in body fluids, has gained the attention of researchers. Ji *et al.* studied a pH-responsive highly diffusive Janus MNM that was functionalized with glucose oxidase (GOx) and a polydopamine (PDA)-Fe^{3+} chelate on two sides. In a glucose-containing solution, the GOx on one side of the MNMs catalyzes the decomposition of glucose into gluconic acid and H_2O_2, enabling a movement speed of 2.67 μm/s [18]. However, some researchers argue that the rate of glucose decomposition catalyzed by GOx is excessively low, and effective propulsion of MNMs can only occur when the glucose concentration within the system is significantly higher than physiological levels. On the other hand, MNMs driven by urease can function normally in the presence of physiological concentrations of urea [20]. Llopis-Lorente and colleagues developed a urease-driven motor that significantly enhances the intracellular delivery and translation of drugs [21]. Feng *et al.* also investigated an enzymatically propelled pot-like micromotor capable of modulating its motion by sensing the ambient fuel concentration. At low concentrations, the urease within the MNM cavity decomposes urea into CO_2 and NH_3, which further convert into ionic species in aqueous solution: NH_4^+, HCO_3^-, CO_3^{2-}, and OH^-. These ions propel the system through ionic diffusion electrophoresis. As the concentration increases, the rapid accumulation of reaction products promotes the formation of CO_2 and NH_3 microbubbles, driving the system through bubble recoil propulsion. Markedly enhanced propulsive force is observed at physiological urea concentrations [22].

Increasing evidence strongly suggests the valuable advantages of enzymes in the field of biomedicine. However, the practical application of enzymes is limited by their inherent variability and susceptibility to deactivation. To address this issue, researchers often employ the technique of encapsulating enzymes within nanomaterials for protective purposes. By anchoring enzymes onto nanoscaffolds, enzymatic reactions can be stimulated, enabling MNMs to demonstrate autonomous motion under mild conditions. This approach not only maintains excellent biocompatibility and stability but also minimizes the risk of

enzyme deactivation. Metal–organic frameworks (MOFs) represent a unique category of composite materials that possess characteristics such as high porosity, large surface area, good biocompatibility, and chemical stability [120]. These properties make them easily customizable and perfect for accommodating biomacromolecules or live cells [101]. Moreover, modifying the power unit onto MOF structures and loading drugs onto them is a commonly used method for constructing therapeutic MNMs. For example, researchers have successfully anchored GOx, catalase (CAT), and the photosensitizer chlorin e6 onto a platinum prodrug-based ZIF framework [15]. Many nanomaterials protect enzymes and can also have negative effects on enzyme activity, leading to a decrease in the self-propulsion rate of MNMs. To address this problem, Kaang *et al.* proposed a solution by achieving optimal conditions through the modulation of the input ratios (Pdop, ZIF-8, and enzyme). This adjustment influences the multilayer laminar flow, resulting in the synthesis of the Pdop@urease@aZIF-8 MNMs. This MNM displays enhanced catalytic activity compared to batch-produced crystalline MNMs due to its facilitated interaction with urea through mesopores. Consequently, the resulting MNMs exhibit outstanding performance in photothermal ablation without compromising enzyme activity [23].

After successful development of an efficient delivery system under controlled experimental conditions, numerous challenges remain to be overcome. When MNMs enter the microenvironment, they encounter clearance mechanisms. Additionally, those engulfed by lysosomes require timely escape to perform subsequent tasks effectively. An innovative solution for future development lies in the combination of the potent catalytic performance of enzymatic reactions and the adaptability of inorganic catalysts to the environment. This allows for the creation of dual-driven MNMs that fully utilize the characteristics of both systems.

In one study, a layer-by-layer (LbL) self-assembly technique was used to coat calcium carbonate NPs with polyethyleneimine (PEI) and CAT, resulting in the formation of MNMs. Folic acid was attached to PEI as a tumor-targeting component, while the catalytic layer of CAT generated thrust. Although the enzyme-driven propulsive component was disrupted upon cellular uptake, the degradation of $CaCO_3$ led to the release of PEI and the proton sponge effect induced by CO_2. This facilitated the escape of the MNMs from lysosomes to the cytoplasm, significantly improving their effective payload capacity [100]. This synergistic strategy represents an adaptive solution for complex microenvironments in current MNM delivery systems. These findings warrant further in-depth and sophisticated investigations by researchers in the future.

Enzyme-driven MNMs show great potential in enhanced propulsion. However, their practical application is limited by drawbacks such as low stability and inactivation. The aforementioned strategies of encapsulating with nanomaterials or combining with inorganic materials have proven effective. In addition, the synergistic application of enzymatic and non-enzymatic techniques presents another viable solution. Further research is needed to develop protective measures or structural modifications for enzymes that do not compromise catalytic efficiency for addressing the challenges posed by complex *in vivo* environments.

2.1.2 External field driven

External field-driven propulsion offers a promising solution to the challenges posed by using chemical reactions for energy production within the microenvironment. There are several drawbacks to relying solely on chemical reactions, including the potential adverse effects of the generated substance concentration gradient or fuel on the organism. The concentration of substances under physiological conditions is often limited within a certain range, which may not provide sufficient power for MNMs. Furthermore, the design of MNMs and control over their direction are constrained by the microenvironment.

External field propulsion overcomes these challenges by providing energy without introducing new substances, ensuring safety and reliability. Additionally, the parameters of external fields can be adjusted, enabling precise control over the magnitude and direction of the energy supply. As there is no longer a need for direct interaction with the internal environment, the design possibilities for MNMs have become more versatile.

Current research in this area includes various external field propulsion methods, including light propulsion, magnetic propulsion, electric field propulsion, and US propulsion, among others.

2.1.2.1 Light

Light, a widely utilized clean energy source, is a promising propulsion mechanism for MNMs through photodriving. Photodriving offers enhanced flexibility in comparison with other energy-driven MNMs because light can be controlled not only by its intensity but also by its direction, wavelength, and polarization. Therefore, light serves not only as a power source but also as a control signal for the targeted motion of MNMs [121,122]. Initially, ultraviolet (UV) radiation was investigated as the energy source for light propulsion. Under UV irradiation, TiO_2 catalyzes a

complex cascade of radical chain reactions in water, converting light energy into mechanical energy to propel MNMs *via* diffusiophoresis [31]. Researchers are also exploring visible light propulsion, which involves engineered rod-shaped MNMs undergoing self-electrophoresis under specific illumination conditions [32,33]. Additionally, light can induce photochemical reactions, resulting in an asymmetrical distribution of bubbles [34]. Furthermore, photochromic reactions can alter the chemical structure or interfacial properties of materials, generating tension gradients to drive the motion of the system [35].

Near-infrared (NIR) light is commonly used as an energy source due to its strong biopenetration capabilities. MNMs asymmetrically loaded with photothermal agents generate thermal gradients under NIR irradiation, driving autonomous motion. Liu *et al.* conjugated the Alzheimer's disease therapeutic factor Aβ-targeting peptide inhibitor D-RK10 (D-RTHLVFFARK) onto the gold hemispheres of silica NPs. NIR irradiation of Au generates the power needed for motion. Substances loaded onto MNMs move with their motion, and molecules in the solution become activated due to the nanomotor's movement. This approach enhances the therapeutic efficacy of NIR-driven MNMs [36]. MNMs loaded with photothermal therapy (PTT) agents can generate localized heat through photothermal effects, achieving efficient PTT. PDA is the most commonly used photothermal agent for constructing such systems. Gui *et al.* used a NIR-driven PDA MNMs loaded with copper ions (JMPN@Cu2) to treat chronic limb ischemia. The photothermal effect and copper ions facilitated vascular regeneration in the ischemic hind limbs. The antioxidative and anti-inflammatory properties of the PDA substrate also reduced the cytotoxicity of Cu^{2+}, improving the ischemic microenvironment [37]. Light-driven MNMs often integrate PTT, photodynamic therapy (PDT), and chemical drugs to form a multipathway therapeutic platform, enhancing treatment efficacy. Ji *et al.* reported a parachute-shaped MNMs propelled by NIR light (PMN-MN) with platinum nanoparticles (PtNPs) serving as photothermal agents. By leveraging hydrophobic interactions, miconazole nitrate (MN) can be effectively loaded onto the canopy of PMNs. Through synergistic PTT and drug treatment, PMN-MNs demonstrated promising therapeutic effects against *Candida albicans* and fungal biofilms *in vitro* [38].

However, light-driven MNMs face challenges such as intermittent light exposure and temporary motion pauses, significantly affecting their delivery capabilities. Zhang *et al.* utilized the unique optical phenomenon of persistent luminescence (PL) and proposed the use of US to activate mechanoluminescent materials. These materials can rapidly store excitation energy in electron holes and emit sustained fluorescence over several days. US treatment generates PL emission as an internal NIR source, continuously exciting the PDA caps and inducing mild photothermal effects on tumors [39]. The efficacy of light-driven MNMs is influenced by tissue transparency, necessitating light-shielding measures during fabrication and storage, which limits their applicability and increases costs. Integrating an internal light source within the system eliminates the need for a continuous light supply and relaxes storage requirements, potentially representing a future development trend. However, addressing the issue of poor controllability is crucial before widespread adoption. Future research on light-driven MNMs may advance toward effects on single cells while also focusing on reducing their costs [121].

2.1.2.2 Magnetism

The propulsion of magnetic MNMs relies on the alignment between magnetic components and the magnetic field. During the construction process, the selection of magnetic responses includes a range from ferromagnetism and paramagnetism to diamagnetism. The magnetic fields involved include uniform magnetic fields (with constant intensity and direction in both space and time), non-uniform magnetic fields (where intensity varies with position but remains constant over time), rotating magnetic fields (with direction changing over time), and oscillating magnetic fields (with intensity varying over time) [123].

Compared to other propulsion methods, magnetically propelled MNMs constructed from magnetic materials offer the distinct advantage of remote and precise control over the position, orientation, and velocity of the MNMs by adjusting the parameters of the magnetic field. This capability facilitates targeted delivery to cancer cells. For the first time, Gao *et al.* achieved high-speed transportation of chemotherapeutic drugs to HeLa cancer cells using fuel-free magnetic-driven MNMs [42].

In magnetic NP research, magnetite (Fe_3O_4) is a widely utilized magnetic iron oxide. Many targeted delivery systems for chemotherapeutic drugs based on Fe_3O_4 NPs have been developed, and these systems exhibit superior specificity for human cancer cells and drug release rates [43]. Recently, carbon nanocomposites, such as cellulose nanocrystals (CNCs)/Fe_3O_4 MNMs synthesized through innovative synthetic approaches, have been introduced. These MNMs exhibit controllable individual or clustered motion under the influence of external direct current or rotating magnetic fields, facilitating targeted drug delivery to single cells or cell clusters [44].

Additionally, magnetic propulsion possesses the unique advantage of enabling the retrieval and recycling of MNMs, which can be leveraged for reuse and pollution removal [124]. Wang *et al.* reported a novel modification of Fe_3O_4 NPs using meso-2,3-dimercaptosuccinic acid (DMSA), termed Fe_3O_4@DMSA. This active mobility increases the probability of interactions between magnetic MNMs acting as adsorbents and Pb(II)-contaminated hemoglobin (Hb). Upon adsorption, these entities can be further separated from the bloodstream through magnetic field-assisted isolation [45]. Due to their recyclable nature, these materials are widely applied in wastewater treatment, which will be described in the application section.

Theoretically, magnetic propulsion can regulate the posture and behavior of magnetic MNMs by altering the characteristics and parameters of the magnetic field. However, the lack of effective real-time monitoring methods for their operation within biological systems hampers further manipulation, thereby limiting the development of such MNMs. Wang *et al.* utilized US imaging to monitor the movement of magnetically controlled MNMs [125]. Although the imaging resolution of this study was low, it provides a potential solution for real-time tracking. Another question is that in designing magnetic MNMs, the magnetic components frequently involve non-biocompatible materials, and the fabrication process is often complex, which increases production costs and technical challenges. Additionally, further research is needed to explore their long-term biocompatibility and biodegradability.

2.1.2.3 US

In the field of MNM construction, US has gained significant attention from researchers due to its non-invasive nature, rapid triggering speed, substantial thrust, and scalability. The team led by Wang was the first to develop metallic rod propulsion using US [25].

The underlying principle of acoustic propulsion lies in the interaction between US and NPs suspended in a fluid. This interaction leads to various motion behaviors of the particles due to the frequency and intermittent nature of the US [126]. Acoustic propulsion can be categorized into two main types: acoustic standing wave propulsion and acoustic droplet vaporization propulsion. Acoustic standing wave propulsion involves the interaction between US-induced fluid motion or density variations and asymmetric structures to propel MNMs. On the other hand, acoustic droplet vaporization propulsion is induced by the momentum increase of MNMs through droplet evaporation [127].

High-intensity-focused ultrasound (HIFU) has demonstrated remarkable biological effects in clinical disease treatment. Yu *et al.* developed an acoustically propelled ferroptosis MNMs based on HIFU-induced cell death. By incorporating perfluorooctyl bromide, the MNMs become responsive to HIFU, leading to the creation of HIFU-driven MNMs (NP-G/P). These MNMs have been successfully utilized in the treatment of triple-negative breast cancer [26]. Additionally, low-energy US has been widely applied in non-invasive imaging [128].

Research on US-propelled MNMs has focused mainly on gold nanowires (AuNWs). For example, Zhang *et al.* developed a red blood cell (RBC)-perfluorocarbon oxygen delivery system using the excellent biocompatibility of AuNWs and their responsive nature to US. This system facilitated the transportation of oxygen to J774 macrophages [27]. In another study, Bhuyan *et al.* employed US-driven MNMs to alleviate intracellular oxidative stress and amyloidogenic degradation. These MNMs, synthesized from unfermented tea buds of the *Camellia sinensis* plant, offer improved biocompatibility compared to their synthetic counterparts [28].

Recent studies have indicated that US can not only act as a power source for propelling MNMs (NMs) but also serve as a trigger for US-dependent sonodynamic therapy (SDT) [129]. This therapy triggers the production of abundant singlet oxygen ($^1O_2$), leading to cell apoptosis. Furthermore, US has been found to induce immunogenic cell death (ICD), which promotes the release of tumor-associated antigens (TAAs) and damage-associated molecular patterns (DAMPs), activating the body's antitumor immunity [130].

Cao *et al.* successfully achieved targeted drug delivery by functionalizing chondroitin sulfate (CS) ligands on the surface of colon tumor cells with CD44 glycoproteins. When combined with US irradiation and oral administration, the CS-ID@NM/hydrogel system is able to traverse the gastrointestinal tract and release NMs in the colon. These nanomaterials are specifically taken up by colon tumor cells through CS ligand (CD44)-mediated endocytosis. Once internalized, the Mn^{2+} released from NMs catalyzes the breakdown of endogenous H_2O_2, resulting in the generation of hydroxyl radicals (˙OH) and O_2. This process initiates a Fenton-like reaction, synergistically killing tumor cells through chemodynamic therapy (CDT) and SDT [24].

Similarly, a study explored the use of a sensitizer activated by US to produce toxic free radicals, disrupting cell structures and inducing apoptosis. The release of 2,2′-azobis [2-(2-imidazolin-2-yl)propane] dihydrochloride by MNMs has been shown to simultaneously generate nitrogen gas and cytotoxic free radicals, enabling synergistic SDT and gas therapy [29]. The unique biological effects of US make it a valuable tool in propulsion methods, especially in the field of tumor therapy. Future research endeavors can focus on investigating the potential of US in the management of other diseases.

Ultrasonic propulsion is a versatile and highly penetrative method for driving MNMs in biomedical applications. The design and fabrication of US-responsive components pose significant challenges, which are common concerns in the development of such structures. In addition, the propulsion mechanisms are still unclear. Suzanne Ahmed *et al.* proposed an US-driven self-acoustic electrophoresis mechanism, which suggests that the acoustic pressure gradient can be utilized to drive MNMs [131]. However, subsequent studies have observed motion directions that do not align with theoretical predictions, although they are consistent with the acoustic streaming model developed by Nadal and Lauga [132]. These issues collectively limit the further development of US-propelled MNMs.

The ability of MNMs to combine propulsion with SDT offers significant potential for synergistic treatments. However, US-based MNMs still encounter challenges such as low propulsion efficiency and the potential for capillary rupture and platelet activation [133,134]. Further investigation into the biological effects of US is warranted to guarantee its security while simultaneously improving operational precision and efficiency.

2.1.3 Synergistic-driven

The use of MNMs powered by external sources presents challenges due to equipment and environmental requirements, limiting their applicability in emergency situations and long-term therapeutic maintenance. Moreover, the impact of external fields on deep tissues decreases with increasing depth.

To address various issues, such as insufficient power in MNMs that rely on a single energy source, strict equipment constraints, and limited adaptability to complex microenvironments, researchers have explored the construction of MNMs using a hybrid energy supply approach. These studies aimed to enhance the adaptability of MNMs platforms to complex environments by employing different driving mechanisms interchangeably and in combination [135]. Recently published synergistic-driven MNMs and their size, motion speed, propulsion mechanism, and applications are summarized in Table 3. Gao *et al.* reported on a hybrid-powered MNM that combines redox reactions with a physical field. In this structure, Pt-Au catalyzes redox reactions, while Au–Ag-flex Ni is used for magnetic propulsion. By switching between propulsion modes, this system effectively addresses the common issues of fuel shortages and ion quenching at high concentrations encountered in chemically powered MNMs [136]. Additionally, flexible integration of dual physical fields is

Table 3: Comparative analysis of MNMs and their biomedical applications (synergistic-driven)

Function carrier	Size	Motion speed	Propulsion mechanism	Applications	Ref.
t-Au-Ag-Ni	—	8 μm/s	Magnetism-bubble propulsion	—	[136]
Au–Ni–Au	300 nm in diameter and 4.5 ± 0.3 μm in length	20 μm/s	Magnetism-ultrasound propulsion	Treatment vascular obstruction	[137]
CD-LA-Au-aV	250 nm	5–8 μm/s	Light-bubble propulsion	Treatment atherosclerosis therapy	[138]
HAPA@Dox	337 ± 13 nm	60 μm/s		Treatment tumor	[139]
Poly(ε-caprolactone)	230 nm	3.95 μm/s		Treatment tumor	[140]

"–" means no given data in the references.
aV: anti-VCAM-1 antibody, HAPA: HMSNPs@ABC@PDA@Au.

considered a promising direction for future construction efforts. In one study, US facilitated linear translational motion, while magnetic control enabled rotational movement, thereby allowing independent direction and control of individual components [137].

Conversely, the introduction of multimodal driving mechanisms holds promise for overcoming the power limitations inherent in many currently used single-driving-mode MNMs. Chen *et al.* developed a fuel-carrying MNM. Using hollow mesoporous silica nanoparticles (HMSNPs) coated with PDA as the substrate and loaded with ammonium bicarbonate (ABC), the photothermal effect induced by PDA under NIR light irradiation promotes the decomposition of ABC and propels the system, subsequently releasing CO_2 to drive the motion of the MNMs [139]. The light-bubble propulsion mechanism enables movement at a speed of 60 μm/s. Another study designed microneedle patch MNMs employing a synergistic light-bubble dual-driving strategy. The MNM matrix consisted of sodium HA loaded with luteolin (Le), the photosensitizer indocyanine green (ICG), and the NO donor L-Arg. In this system, the HA component possesses biocompatibility and rapidly dissolves in solution, while Le exerts its antibacterial effect by damaging bacterial cell membranes and inhibiting biofilm formation. ICG and L-Arg serve as the driving components for light-driven and bubble-driven mechanisms, respectively [141]. Wu *et al.* covalently conjugated the NO donor L-Arg) with β-cyclodextrin and attached AuNPs onto the MNM surface. The photothermal conversion properties of Au NPs facilitate the ablation of inflammatory macrophages and provide additional propulsion to the MNMs under NIR laser irradiation, guiding and promoting the aggregation of MNMs within AS plaques [138].

Synergistic-driven propulsion integrates multiple propulsion mechanisms, enabling MNMs to adapt to complex environments. By combining diverse propulsion methods, this strategy shows significant potential for multimodal application platform. Future studies should focus on optimizing hybrid energy systems and investigating the interactions between different propulsion mechanisms to enhance their overall efficiency and performance. The comparison of various driven methods is summarized in Table 4.

2.2 Targeting

To enable accurate cargo delivery and perform biomedical tasks effectively, MNMs are capable of navigating to designated work areas as needed. The distinguishing feature of these MNMs is their targeted motion, which sets them apart from conventional passive transport methods. Currently, the targeting of MNMs is achieved through the use of chemotaxis, bionanoelements, and the modulation of external field parameters.

2.2.1 Chemotaxis

Chemotaxis is the phenomenon in which cells respond to concentration gradients of substances in the extracellular environment, thus resulting in directed movement. In the microenvironment of pathological lesions, there are systematic variations in the concentration and properties of substances as the position deepens. This phenomenon serves as the theoretical foundation for the active movement of MNMs [142]. Studies have reported that GOx-driven MNMs exhibit positive chemotaxis along glucose concentration gradients [143]. Currently, chemotaxis-based targeting is an extensively studied strategy. However, its targeting process faces obstacles such as poor precision, limited controllability, and strong dependency on the working microenvironment, thus impeding its further advancement.

In tumors, the abundant presence of lactic acid is attributed to the robust metabolism of glucose and glutamine by tumor cells. In regions far from blood vessels, tumor tissues do not receive sufficient oxygen supply, resulting in increased lactic acid production in deeper tumor tissues [46]. As a result, a model exists within tumors wherein lactic acid levels are low extracellularly and high intracellularly. Zhang *et al.* developed a novel nanoradiosensitizer (Pt/DOX/LOX/LM cRGD, referred to as PDLR) driven by lactic acid. These multifunctional NPs exhibit positive chemotaxis and self-oxidation properties. Through lactate oxidase (LOX) catalysis, PDLR converts lactic acid into H_2O_2, thereby reducing tumor lactic acid levels. Pt NFs catalyze both exogenous and endogenous H_2O_2, converting them into O_2 to alleviate hypoxia. Additionally, porous Pt-NFs with a high atomic number can undergo X-ray radiation, thereby safeguarding surrounding healthy tissues from radiation effects (Figure 3a) [64]. Researchers have made significant efforts toward constructing chemotactic systems based on the concentration of H_2O_2. Most recently, Yu *et al.* documented that chemotactic micro/NMs are fuelled by H_2O_2, demonstrating movement along the H_2O_2 gradient in the bloodstream toward tumor sites. GOx and Cat were coimmobilized on cationic gold nanoclusters (CAuNCs@HA) [102]. Prodyut Dhar engineered MNMs with the ability to autonomously move in extremely low concentrations of peroxide, leveraging CNCs extracted from bamboo stems. The trajectory of these micromotors

Table 4: Advantages and disadvantages of different driven methods

Driven method	Propulsion mechanism	Advantages	Disadvantages	Characteristics in biomedical applications
Redox reaction driven	—	Self-sufficient, no external energy source is required	The products of redox reactions may be harmful and might impact the composition of the microenvironment	Due to the presence of various characteristic substances and pH levels in the tumor microenvironment, it can provide both fuel for redox reactions and a natural targeting gradient, making it suitable for constructing redox reaction-driven MNMs that operate within this environment. However, it is not well suited for tasks that require high-precision targeting capabilities
		Widely studied and high propulsion efficiency	Low propulsion efficiency under physiological conditions, requiring high fuel concentrations Difficult to precisely control propulsion direction Short continuous propulsion duration	
External field driven	Light	Remotely controllable; motion-adjustable through light intensity, wavelength, and direction switching. Movement with fast speeds	Limited by tissue transparency; restricted penetration depth	Light propulsion can provide additional synergistic therapeutic effects, such as PDT, demonstrating excellent performance in enhancing treatment outcomes. However, due to limitations in tissue transparency, it cannot effectively function at greater depths. Furthermore, it has high requirements for the environment, equipment, and light sources, making it unsuitable for prolonged applications
		Provides photothermal and photodynamic therapeutic effects	Intermittent light exposure affects continuous propulsion High production cost requires light-shielded storage	
	Magnetism	Relatively safe and remotely controllable	Long-term biosafety of magnetic components requires further research	Magnetism-propulsion MNMs possess unique recyclable properties that allow for the reusability of the designed systems. However, they require integration with real-time monitoring systems to function effectively
		Convenient control of movement direction and speed	Expensive materials, manufacturing equipment, and complicated preparation procedures	
	Ultrasound	High penetration depth Fast motion response	Low drug delivery efficiency Potential for capillary rupture and platelet activation	Ultrasonic propulsion is particularly well suited for the development of MNMs intended for deep-tissue applications. However, the precision of this propulsion method is suboptimal, necessitating additional targeting design strategies to compensate in practical applications
		Enhances antitumor effects when combined with sonodynamic therapy	Lack of operational precision	
Synergistic driven	/	Combines multiple propulsion mechanisms, adapting to complex environments	Complex preparation process	Synergistic driven allows for the tailored design of combinations of propulsion methods to meet diverse application requirements, making it one of the most advantageous approaches for practical implementation today
		Enhances targeting efficacy and flexibility	Compatibility of different propulsion requires further study	
		Solves fuel shortage issues with switchable energy sources	Interaction of propulsion mechanisms needs further evaluation	

can be remotely controlled by manipulating the pH gradient [103]. Furthermore, Zhang *et al.* developed a two-dimensional MNM utilizing layered double hydroxide nanosheets. Oxygen bubbles are generated by these nanosheets only in microenvironments where there is a simultaneous presence of slightly acidic/neutral pH and H_2O_2 (characteristic of the tumor microenvironment), thereby exhibiting chemotaxis toward tumors [104]. Baraban *et al.* also observed that catalytic MNMs with tubular and spherical shapes exhibit chemotaxis toward high concentrations of H_2O_2 in microfluidic systems. Leveraging their sensitivity to H_2O_2, studies have indicated that cargo-loaded MNMs can autonomously target specific cells or inflammatory tissues [144].

Chemotaxis-based targeting strategies, although extensively studied, are overly reliant on specific environmental conditions. The disorder of localized substance gradients *in vivo* can disrupt the targeting process, which makes this approach less stable than other targeting methods. For instance, Wang *et al.* encountered the challenge of insufficient local H_2O_2 concentrations to achieve driving and targeting tasks, which prompted the development of Pt–Pd alloy propulsion components to enhance catalytic efficiency [14]. Researchers have actively developed alternative targeting strategies to address these challenges.

2.2.2 External field parameters

The direction and behavior of externally driven MNMs can be controlled by adjusting the parameters of the external field. Precisely modulating the intensity of the energy output enables manipulation of the motor's operational speed to a certain extent. The guidance of MNMs by external fields is closely linked to their propulsion design.

Wang *et al.* reported the development of an enzyme-driven cup-shaped MNM that demonstrates excellent biocompatibility. These gold nanocup (GNC)-Pt materials serve as *in situ* O_2 generators, addressing the limitations of the hypoxic tumor microenvironment in PDT. Moreover, they are capable of actively targeting cells and facilitating synergistic photodynamic/thermal therapy when exposed to NIR laser irradiation (Figure 2b) [145].

In the domain of external physical fields, magnetic fields are widely and flexibly employed to guide the behavior of magnetic MNMs. By manipulating the magnetic moment and magnetization direction of the magnetic field, it is possible to control their motion trajectories [47,48]. Yang *et al.* developed magnetic hematite colloidal motors that exhibit distinct motion behaviors in an external magnetic field. Under a rotating magnetic field, peanut-shaped motors move in rolling mode, while under a cone-rotating magnetic field, the motor can move in swinging mode. By combining these different motion modes, precise manipulation of MNMs can be achieved [146].

2.2.3 Ligand–receptor interactions

In biological systems, ligand–receptor interactions play a vital role. Ligands and receptors possess specific affinities, and various ligand–receptor-mediated biological events have been extensively utilized to construct targeted strategies. These include lectin receptors, Fc receptors, complement receptors, interleukin receptors, lipoprotein receptors, and transferrin receptors [147]. Compared to

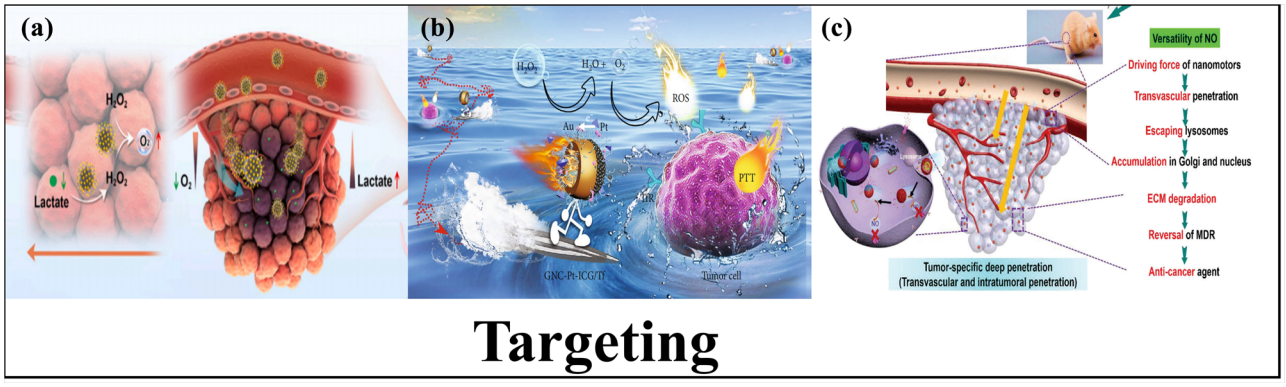

Figure 3: Targeted strategy of nanomotors: (a) Pt/DOX/LOX/LM-cRGD MNMs under lactate gradient exhibits positive chemotaxis *in vivo* and alleviates hypoxia through cascade catalysis from the study by Zhang *et al.* [64]; (b) illustration of NIR-guided GNCs Pt-ICG/Tf nanomotors for synergistic photodynamic/thermal therapy from the study by Wang *et al.* [145]; and (c) tumor-specific deep penetration of HFLA–DOX nanomotors from the study by Wan *et al.* [149]. DOX: doxorubicin; LOX: lactate oxidase; LM: liposomal membrane; NIR: near-infrared; GNCs: gold nanocups; HFLA: heparin/folic acid/L-arginine.

other targeting approaches, ligand–receptor interactions have unique biological compatibility, precision, and multifunctionality, making them indispensable for the future development of MNMs.

Inflammation is characterized by the excessive generation of reactive oxygen species (ROS) stemming from mitochondrial damage, with inducible nitric oxide synthase (iNOS) being predominantly present in inflammatory tissues and scarcely expressed in normal tissues. This significant upregulation indicates the potential of iNOS and ROS (iNOS/ROS) as chemotactic agents for targeted delivery through chemotaxis. Building upon this premise, MNMs loaded with L-Arg can achieve positive chemotaxis along the iNOS/ROS concentration gradient, thereby enabling them to reach the inflamed microenvironment [49]. This concept has also been extended to the design of MNMs utilizing other ligand–receptor pairs for targeting. Fang *et al.* developed a bowl-shaped mesoporous PDA nanomotor that can target thrombi by binding to activated platelet GPIIb/IIIa receptors and RGD [148]. Wan *et al.* utilized heparin/folate NPs with a cage-like structure (acting as an anticancer drug and cancer cell-targeting agent) as carriers loaded with L-Arg and the anticancer drug doxorubicin (DOX), resulting in the formation of HFLA–DOX MNMs. These MNMs can target cancer cells through interactions with overexpressed folate receptors. Simultaneously, L-Arg, *via* dual-ligand hydrogen bonding with the cell membrane, effectively facilitates the cellular internalization of MNMs (Figure 3c) [149]. Recently, Lu *et al.* demonstrated the surface modification of CaO_2 MNMs with the nucleus-specific oligonucleotide AS1411. The oligonucleotide AS1411 can effectively guide MNMs to tumor cells due to its nucleolin protein-specific aptamer characteristics [150].

Furthermore, researchers have harnessed biocell-derived stealth coatings to modify MNMs, emulating the physical, chemical, and biological properties of natural cells. For example, MNMs surface-coated with a macrophage membrane can actively recognize and target macrophages toward cancer cells, thereby enhancing the targeting performance of the MNMs [151]. These MNMs can aggregate at specific sites and extend their residence time in the internal environment by evading immune clearance. While macrophage membrane coatings can enhance targeting specificity, they may also lead to unintended interactions with non-cancerous macrophages or other immune cells, potentially causing off-target effects.

Ligand–receptor interactions usually have high specificity. Its biological nature makes it easy to overcome biological barriers and achieve extended retention time in the body, making it particularly suitable for circulatory applications. However, the irreversibility of biostimulation processes raises concerns about biosafety within the human body.

2.3 Structure

The structure of MNMs can be categorized into two main types: artificial MNMs and biohybrids. Artificial MNMs composed of artificially synthesized materials are currently the most extensively researched type. However, previous studies have faced challenges in terms of biocompatibility and restricted biomedical applications due to the use of non-degradable inorganic materials and polymers [152]. The emerging field of biohybrid MNMs offers a promising direction in structural research, providing researchers with significant performance enhancements and improved task execution efficiency. By incorporating biologically derived components, biohybrid structures aim to address the limitations of artificial MNMs. This can involve adding naturally sourced components to artificial materials or modifying biological components directly to create MNMs. The goal of biohybrid structures is to eliminate immunogenicity, enhance targeting capabilities, and enable specialized tasks [93]. Recently published biohybrid MNMs and their biological components, size, motion speed, energy source, propulsion mechanism, and applications are summarized in Table 5.

One commonly adopted practice is to utilize certain inherent characteristics of natural biological components by conjugating them onto nanoscale carriers. This practice helps to improve structural defects and enhance functionality in MNMs. Inspired by intracellular myosin and actin, Tian *et al.* developed a protein-based motor. They used human serum albumin (HSA), a globular protein found primarily in the circulatory system, as the substrate for constructing MNMs. HSA was chosen for its superior biocompatibility, low immunogenicity, and high solubility. By loading MSO, they were able to inhibit glutamine synthetase enzyme activity in tumor and stromal cells, thereby enhancing ammonia toxicity for effective antitumor therapy [153]. By disguising MNMs with biological structures through biomimicry, immunogenicity and adhesiveness can be reduced, allowing evasion of clearance before reaching the targeted site. The incubation of functional units with bovine serum albumin (BSA) has been shown to effectively prevent phagocytosis by macrophages [140] (Figure 4a). Undesired biological adhesion not only affects task execution efficiency but also hinders the subsequent degradation of MNMs *in vivo*. Cancer cells have significantly reduced adhesion on their surface due to the absence of specific ligands and receptors. Therefore, one promising solution is to construct bionanomotors encapsulated with MCF-7 cancer cell membranes to minimize biological adhesion (Figure 4b) [154].

In addition to improving the biocompatibility of MNMs and providing protection, certain characteristics of biological components can be used to enhance the functionality

Table 5: Structure and function of biohybrid MNMs

Biological components	Size	Motion speed	Energy source	Propulsion mechanism	Applications	Ref.
HAS	250 nm	1.46 $\mu m^2/s$	Redox reaction driven	Self-diffusiophoresis	Treatment tumor	[153]
MCF-7 cancer cell membranes	240 ± 20 nm	6.06 μm/s	External field driven	Light	Cargo delivery	[154]
Extracellular vesicles	126.1 nm	—	Redox reaction driven	Bubble propulsion-NO	Treatment-injured tendon	[155]
DNA	—	—	—	—	Protein therapy	[156]
Brome mosaic virus	25–30 nm	4.15 μm/s	Redox reaction driven	Bubble propulsion-O_2	Cargo delivery	[157]
Sperm cells	—	10 ± 4 μm/s	External field driven	Magnetic	—	[158]
RBC	68 μm	16 μm/s	External field driven	Ultrasound	—	[159]
Escherichia coli (*E. coli*)	600 nm	0.7 ± 0.2 μm/s	Redox reaction driven	Bubble propulsion-O_2	—	[160]

"–" means no given data in the references.
RBC: red blood cell; HSA: human serum albumin.

of MNMs. Liu *et al.* harvested stem cells from the Achilles tendons (AT) of young rats and cultured them *in vitro* to collect extracellular vesicles (EXOs). These EXOs were then loaded into an MN array to prepare MN patches. When the patches degraded, EXO/Methacryloyloxyethyl phosphorylcholine (MPC) and N,N′-bis(acryloyl)cystamine (BAC) and L-arginine was released into the AT microenvironment, facilitating the movement of EXOs toward internal tissues. This mechanism leverages biomimetic properties to accumulate at the injured site [155] (Figure 4c).

Wang *et al.* synthesized MNMs loaded with the nonsteroidal anti-inflammatory drug indomethacin and encapsulated them in 4T1 CCM vesicles. The biomimetic properties of the MNMs allowed for their accumulation at the tumor site [50]. The utilization of other biological components within organisms for constructing drug delivery systems, such as nucleic acids, has gained considerable attention. The precisely controllable structural features and excellent biocompatibility of DNA origami nanostructures have attracted widespread interest. Zhao *et al.* employed this technology for protein therapy by modifying rectangular DNA origami carriers to serve as cancer cell-targeting aptamers. This facilitated the delivery of cytotoxic protein molecules into tumor cells and mediated intracellular RNA degradation (Figure 4d) [156].

Highly ordered biological materials, such as virus-like particles, exhibit stable chemical properties, strong modifiability, and suitable structures for efficient loading. Tejeda-Rodríguez *et al.* pioneered the development of artificial virus-based MNMs using Brome mosaic virus and cowpea chlorotic mottle virus. These MNMs have one side coated with Pt for the catalysis of H_2O_2 [157].

Cell-based biohybrid MNMs have been a significant area of focus in research for quite some time. Specifically, non-pathogenic bacteria, such as *Escherichia coli* (*E. coli*), have been identified as ideal candidates for the development of biohybrid MNMs. In a study by Shanton, *E. coli* was selected for propulsion, and a biohybrid system (Figure 4e) was successfully constructed [161]. Subsequently, *E. coli* was integrated onto metal-coated PS Janus particles, with a specific emphasis on its preferential adhesion to platinum (Pt) metal surfaces. This study sets the foundation for future research endeavors [160]. In biohybrid MNMs, substrates such as nucleic acids, viruses, and cells possess self-replicating capabilities. However, their inability to self-inactivate after completing their intended tasks remains a significant challenge. Utilizing non-proliferative cells, such as RBCs, platelets, or sperm cells, as structural components presents an alternative approach. Magdanz *et al.* developed a bioinspired sperm tube system by integrating sperm cells with coiled magnetic microtubes. This innovation initiated biomedical

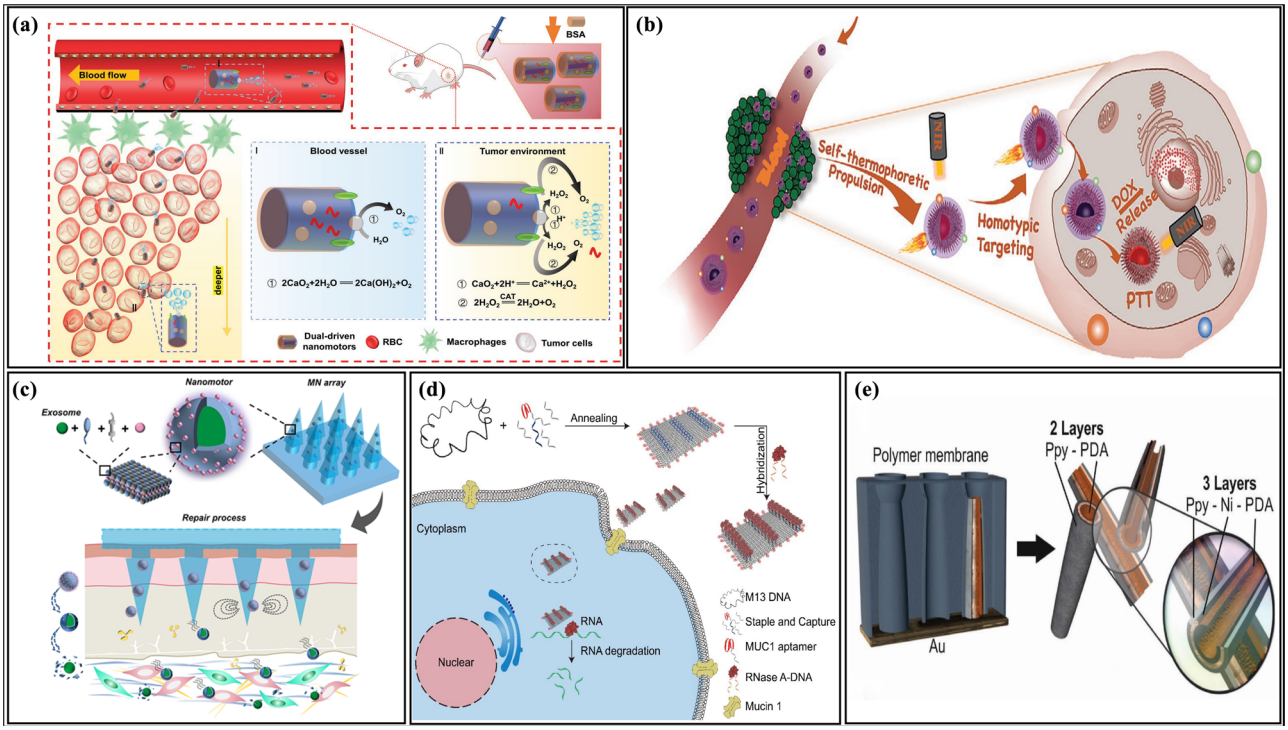

Figure 4: Biohybrid nanomotors: (a) efficiency of dual-power nanomotors driven by different driving reactions in pressure gradient environments from the study by Zheng *et al.* [140]; (b) schematic illustration of active targeting and intracellular internalization of mC@SiO_2@DOX for enhancing photothermal and chemotherapy from the study by Zhou *et al.* [154]; (c) schematic diagram of the preparation and treatment process of EXO/MBA-loaded MN array for Achilles tendinopathy from the study by Liu *et al.* [155]; (d) schematic representation of the self-assembly of functionalized DNA from the study by Zhao *et al.* [156]; (e) schematic representation of the fabrication process of a biohybrid nanomotor based on *E. coli* from the study by Stanton *et al.* [161]. mC: membrane camouflaged; EXO/MBA: exosomes modified by a NO nanomotor.

research applications focused on the controlled guidance of individual cells [158]. The treatment system built upon this concept has found wide applications in cancer treatment [162]. By harnessing the intrinsic properties of RBCs, Wu *et al.* successfully conferred active motility upon them. Through the asymmetric loading of iron oxide NPs into RBCs and the creation of a pressure gradient using US, the RBCs exhibited efficient and sustained motion but remained unaffected by the immune system and internal environment [159]. Characterization results further reveal that these MNMs have an average size of 68 μm, with a motion speed of 16 μm/s, demonstrating superior mobility capabilities compared with other biohybrid MNMs. A recent study has demonstrated the screening and direct binding-efficiency measurement of biological binders (such as antibodies) at the single-bacterial level [163]. This breakthrough offers potential advancements in the design and preparation of biohybrid MNMs.

However, the safety of biohybrid structures has been the subject of ongoing controversy. The injection of biological components into the body can trigger immune reactions and disruptions. The complex mechanisms involved also pose potential biological risks. Further detailed research and assessments are necessary before these structures can be applied in clinical practice.

3 Applications

Currently, MNMs have been widely applied in various domains, yielding promising and potentially scalable results. Here, we highlight four of the most promising and potentially scalable applications: cargo delivery [164], cancer therapy [153], biosensing and imaging [76], and environment restoration [165]. Medical platforms based on MNMs are evolving toward multifunctionality, holding promise for simultaneous disease diagnosis, treatment, and prognosis assessment in the future.

3.1 Applications in biomedicine

3.1.1 Cargo delivery

In the past, researchers have made significant efforts to prepare nanomaterials and develop delivery systems.

The advancement of MNMs has greatly influenced targeted delivery. Building personalized delivery systems for targeted transport based on MNMs, guided by application scenarios, is currently a pivotal area of research. The efficiency of cargo delivery tests the comprehensive capabilities of MNM systems, with advancements in this field poised to rapidly expand into other areas. Thus, cargo delivery constitutes "cornerstone" research in this field. MNMs have been used for the effective delivery of chemical drugs (Figure 5a) [166], antibiotics [136], live cells [160,167], signaling molecules [98], nucleic acids [168], and other substances. Among these, the most extensively researched area is the delivery of chemotherapy drugs.

In summary, achieving more effective delivery involves focusing on robust mobility, secure cargo loading, traversing biological barriers, and efficient cellular internalization of MNMs. Ensuring the safety and efficiency of cargo transportation is of utmost importance during the transport process.

Appropriate dimensions play a crucial role in facilitating the evasion of immune surveillance and renal clearance by MNMs, thus ensuring the secure protection of cargo [169]. Previous research on multidrug delivery for cancer treatment has focused primarily on conjugating or encapsulating/modifying drugs with active molecules on nanocarriers. In the context of cancer chemotherapy, studies have demonstrated significant advantages, including a high drug payload, minimal side effects, prolonged drug retention time, and high tumor suppression rates. However, these methods suffer from mutual interference, lack of controllability, and suboptimal safety. Researchers argue that an ideal delivery system should be able to load different drugs without interference and possess robust modifiability for further design [166]. Wang *et al.* employed an "epitaxial growth" method (Figure 5b) to concurrently construct a mesoporous/macroporous composite structure. By appropriately restricting the macropore size, PtNPs were anchored within the range of 20–40 nm, thereby enhancing their stability. Under NIR irradiation,

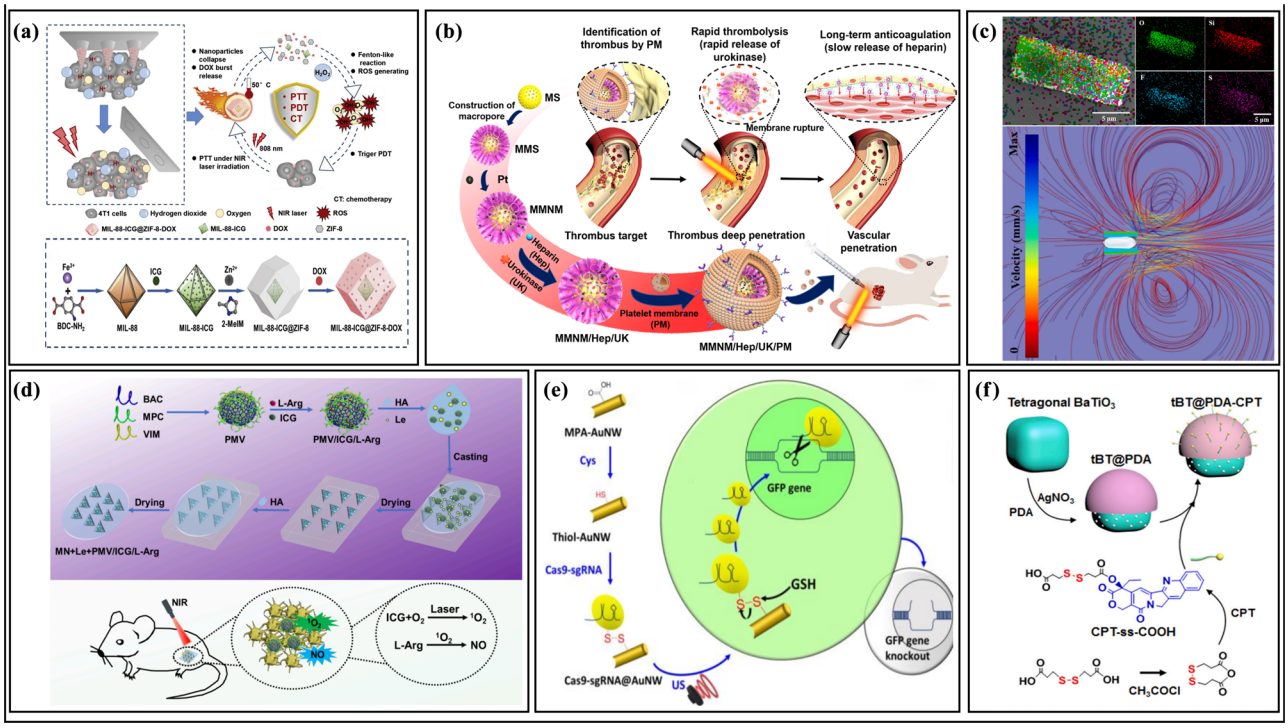

Figure 5: Applications of nanomotors in biomedicine: cargo delivery: (a) schematic diagram of MIL-88-ICG@ZIF-8-DOX nanomotor synthesis (bottom) and its application in synergistic photothermal/photodynamic/chemotherapy treatment of tumors (top) from the study by Wu *et al.* [166]; (b) schematic diagram of MMNM/Hep/UK/PM nanomotor synthesis and its mode of action in the process of thrombus treatment from the study by Wan *et al.* [55]; (c) EDS elemental mapping of a PEDOT-SiO_2 micromotor (top) and the trajectory pattern of particle motion around micromotor (bottom) from the study by Lu *et al.* [171]; (d) schematic diagram illustrating the preparation process of micro-needle patches and the mechanism of antibacterial therapy from the study by Chen *et al.* [141]; (e) schematic illustration of Cas9–sgRNA delivery approach from the study by Hansen-Bruhn *et al.* [168]; and (f) schematic representation of the preparation process for Janus tBT@PDA-CPT NPs from the study by Meng *et al.* [59]. MMNM/PM: mesoporous/macroporous silica/platinum nanomotors with platelet membrane; Hep: heparin; UK: urokinase; EDS: energy-dispersive X-ray spectroscopy; PEDOT: poly(3,4-ethylenedioxythiophene); tBT: tetragonal $BaTiO_3$; PDA: polydopamine; CPT: camptothecin.

sequential drug release was achieved, including rapid release of urokinase (within 3 h) and sustained release of heparin (>20 days), exerting long-term control effects on thrombosis [55].

Given the complexity of biological fluids, MNMs require robust motility and controlled motion [170] to carry out delivery tasks effectively. To meet these requirements, Lu *et al.* developed a tubular hydrophobic poly(3,4-ethylenedioxythiophene) (PEDOT)/SiO_2 micromotor (Figure 5c) capable of ultrafast motion activated by US. In the absence of any chemical fuel, trapped bubbles within the micromotor resonate with US, sustaining the spontaneous propulsion of the PEDOT-SiO_2 micromotor. The micromotor achieved a maximum velocity of 1,100 body lengths per second [171].

The presence of various biological barriers within organisms, along with the inherent complexity of the microenvironment, has long been a significant factor contributing to the inefficient delivery of cargo. MNMs, by leveraging their motility, play a crucial role in traversing and penetrating these barriers to facilitate cargo transport. Both propulsion mechanisms and the structural characteristics of MNMs can influence traversal efficiency.

The formation of biofilms by bacteria is a critical factor in the development of antibiotic resistance and is a significant contributing factor to various bacterial infectious diseases. To address this issue, Maric *et al.* devised an infrared light-driven mesoporous SiO_2/Au MNMs to eradicate *Pseudomonas aeruginosa* biofilms. Experimental evidence has demonstrated that this MNMs exhibit robust photothermal ablation capabilities for bacterial biofilms [172]. In another antibacterial system, the MNM matrix consisted of sodium HA loaded with Le, the photosensitizer ICG, and the NO donor L-Arg (Figure 5d). The HA rapidly dissolves in solution, while Le exerts its antibacterial effect by damaging bacterial cell membranes and inhibiting biofilm formation [141].

Gao *et al.* designed a zinc-based MNM that reacts with acid in gastric fluid, generating bubbles that propel the MNMs to rapidly traverse the gastric mucus layer [173]. Peng *et al.* developed polymer vesicle MNMs based on poly(ethylene glycol) (PEG)-b-PS and poly(acrylic acid)-b-PS, which exhibit tunable sizing capabilities. In tumor vascular model systems, these sub-200 nm MNMs can prolong circulation time and effectively traverse the vascular endothelium. Importantly, the ability to make flexible adjustments according to application requirements is a crucial aspect for future development [174].

The bladder wall is covered by a mucosal layer containing glycosaminoglycans (GAGs). GAGs serve as antibacterial coatings for the bladder, inhibiting the attachment of pathogens. However, they also impede the delivery of therapeutic drugs. Choi *et al.* reported a high-bioavailability MNM that addresses this issue by relying on the high urea content in the bladder to convert urea into carbon dioxide and ammonia, thereby driving the MNMs to penetrate deeply into the mucosal layer of the bladder wall [56]. Recently reported pluronic F127 (P127)-modified gold-shell (AuS) polymeric core NPs were loaded with the anti-inflammatory drug curcumin. These NPs are capable of traversing the colonic mucosal layer under NIR irradiation and accumulating within the mucosa for the treatment of ulcerative colitis (UC) [57].

The cell membrane protects cells from the intrusion of toxic substances, but also impacts the absorption of drugs and beneficial compounds [175]. The translocation of MNMs across the cellular membrane relies on the interaction between ligands and receptors present in their structure. Reports indicate that US-propelled MNMs loaded with Cas9–sgRNA complexes can directly penetrate the cellular membrane of GFP-expressing B16F10 cells, leading to continuous intracellular release of Cas9–sgRNA and thereby enhancing gene knockout efficiency by 50% (Figure 5e) [168].

Magnetic-driven and redox-responsive nanocarriers for intracellular protein delivery, functionalized with the transmembrane peptide TAT, significantly enhance the efficiency of MNM penetration across the cell membrane [58]. The success rate of cellular internalization has a significant effect on the effectiveness of drug action. Enhancing cellular uptake efficiency by modulating the membrane potential and permeability of cancer cells is a well-established and effective strategy. Meng *et al.* developed a MNM called tBT@PDA-CPT (Figure 5f) by encapsulating camptothecin (CPT) grafted with PDA on pyroelectric tetragonal $BaTiO_3$ (tBT) NPs. When exposed to NIR irradiation, the PDA layer on tBT NPs induces temperature changes, leading to spontaneous polarization and redistribution of surface charges. By leveraging the membrane potential disparity between tumor and normal cells, thermoelectric NPs generate microcurrents that modulate membrane fluidity and promote endocytosis [59]. This strategy has also been extended to antimicrobial therapy by loading ciprofloxacin onto a PDA cap, resulting in tBT@PDACipNP [60]. Zhao *et al.* also achieved enhanced cellular internalization using piezoelectric materials [61].

3.1.2 Tumor therapy

MNMs loaded with therapeutic components have been utilized along with strategies such as conventional chemotherapy, physical tumor ablation, and modulation of

the tumor microenvironment to inhibit tumor growth. MNMs serve as versatile tools that are integral to various stages of tumor therapy. The recently published tumor therapy MNMs, along with their energy source, construction, treatment mechanisms, and the tumors they target for treatment, are summarized in Table 6.

The microenvironment of lesions plays a significant role in disease treatment and prognosis. On the one hand, it affects the process and effectiveness of drug action at the site of the lesion. It is characterized by the dependency of pathological–physiological cascades on the components within the microenvironment. Manipulating the lesion microenvironment by removing or adding specific small molecules to treat disease, improving patient prognosis, and enhancing therapeutic outcomes is also an important application of MNMs in the biomedical field. The tumor microenvironment is a highly structured ecosystem that exhibits distinct characteristics at different stages of various tumors [176]. MNM delivery systems have been developed based on specific features of tumor microenvironments, such as hypoxia, high lactate levels, elevated interstitial pressure, and low pH.

The complex tumor microenvironment and abundant connective tissue are significant factors contributing to the limited efficacy of drug delivery systems. The absence of lymphatic vessels and impaired lymphatic drainage in the tumor stroma cause fluid retention, hindering the penetration of drugs into the tumor. Fu *et al.* developed a MNM (Figure 6a) with the ability to undergo redox reactions with moisture in the tumor stroma under NIR excitation. This process generates oxygen (O_2), effectively degrading the main component of stromal fluid, water. As a result, tumor interstitial pressure is significantly reduced, enabling more effective subsequent treatments [63].

Lactate plays crucial roles in tumor proliferation, metastasis, and drug resistance. To address hypoxia and eliminate lactate, Zhang *et al.* created a multifunctional nanoradiosensitizer (Pt/DOX/LOX/LM-cRGD, referred to as PDLR) with positive chemotaxis and autoxidation capabilities. By utilizing LOX, PDLR catalyzes the conversion of lactate to H_2O_2, thereby reducing lactate levels within the tumor [64].

Interestingly, some researchers have leveraged the accumulation of lactate within cells to inhibit tumor growth. Wang *et al.* presented PCA (PSBMA/L-Cys/α-CHCA) (Figure 6b), where L-Cys, catalyzed by CBS in the tumor microenvironment, generates H_2S to provide energy. This process leads to abundant lactate production, inhibiting intracellular proton efflux and causing tumor cell acidosis. Simultaneously, α-CHCA suppresses the expression of MCT-1/4, disrupting the transfer of lactate between tumor cells and leading to excessive intracellular lactate accumulation, ultimately exacerbating acidosis [65].

Harnessing the host immune system for disease treatment represents an effective and versatile approach. Immunotherapy involves inducing the host's immune response rather than delivering exogenous drugs to tumor lesions, thereby eliciting the killing of cancer cells. Wang *et al.* developed light-propelled asymmetric hydrogel MNMs by coupling hydrogels with copper sulfide. Upon entry into the lesion, the MNMs loaded with DOX and dopamine exert enhanced immunotherapy effects and release DOX for chemotherapy. Dopamine facilitates the capture of DAMPs and TAAs at the tumor site, assisting their interaction with immature dendritic cells (DCs) to promote DC maturation. Mature DCs facilitate antigen presentation, initiating a specific immune response to hinder tumor progression [66].

Ferroptosis, a programmed cell death pathway, is initiated by the catalysis of Fe^{2+} or lipoxygenase on unsaturated fatty acids in the cell membrane, leading to lipid peroxidation and subsequent apoptosis. In comparison with normal tissues, the tumor microenvironment harbors elevated levels of ROS, rendering it more sensitive to ferroptosis. Liu *et al.* engineered an MNM based on the MOF material NH2-MIL-101 asymmetrically loaded with PEG and glutathione hydrolase gamma-glutamyltransferase (GGT). Among these MNMs, GGT effectively inhibits the synthesis of glutathione (GSH), alleviating its interference with ferroptosis while simultaneously generating Fe^{2+}. The involvement of Fe^{2+} in Fenton reactions produces an excess of ROS, further promoting the death of tumor cells (Figure 6c) [67]. Under specific conditions, Mn^{2+} can also exert this effect [68].

Despite significant advancements in tumor therapy based on ferroptosis mechanisms, critical issues remain to be addressed. Researchers are exploring combination therapy strategies based on ferroptosis to compensate for the shortcomings in tumor eradication rates associated with ferroptosis alone. Zhang *et al.* reported a light-driven nanodelivery system (Figure 6d) for photothermal-enhanced ferroptosis therapy in tumors. Upon uptake by tumor cells, Fc and Hb catalyze the generation of toxic $^{\cdot}OH$ under the influence of H_2O_2. Hb also depletes GSH, leading to GPX4 enzyme inactivation, resulting in lipid peroxide accumulation and further induction of ferroptosis [69].

As previously discussed, single-tumor treatment strategies often yield unsatisfactory results. As a result, an increasing number of researchers are inclined toward employing comprehensive therapies based on MNMs, particularly the combination of PTT with other modalities such as chemotherapy, PDT, and immunotherapy [177]. Phototherapy consists of PTT and PDT. PTT utilizes light-absorbing materials to generate heat and induce cancer

Table 6: Treatment mechanism and construction of tumor therapy MNMs

Energy source	Construction	Treatment mechanism	Tumor	Ref.
Redox reaction driven	*In situ* growth of Ag_2S NPs on ultrathin WS_2 nanosheets	Reduce tumor interstitial pressure	Osteosarcoma K7M2-WT tumors, cervical cancer U14 tumors, pancreatic cancer PAN02 tumors	[63]
Redox reaction driven	Loading DOX and modifying LOX (lactate oxidase) on Pt-NFs, followed by coating with lipid membrane decorated with cRGD (LM-cRGD)	Chemotherapy and clear lactate	Breast cancer	[64]
Redox reaction driven	After free radical polymerization of sulfobetaine methacrylate, L-Cys and α-CHCA were loaded.	Acidosis	Breast cancer	[65]
Light	Asymmetric modification of Fe_3O_4@Cu_9S_8 NPs and dopamine onto the asymmetric hydrogel (AHNM)	Chemotherapy and immunotherapy	Breast cancer	[66]
Redox reaction driven	MOF material NH2-MIL-101, asymmetrically loaded with PEG and glutathione hydrolase GGT	Inducing cell apoptosis	Breast cancer	[67]
Light	Concomitant loading of hemoglobin and ferrocene onto the surface of bowl-like PDA NPs	Photothermal ablation and inducing cell apoptosis	Breast cancer	[69]
Light	Modification of PDA was achieved using methoxy polyethylene glycol amine (mPEG-NH2), followed by loading of Dox	Chemotherapy and PDT	Breast cancer	[71]
Light	Coating ZIF-8 onto UCNPs to prepare a core–shell structure for loading photosensitizers, catalase, and glucose oxidase	PDT and starvation therapy	Cervical cancer	[72]
Light	—		GBM	[73]
Light	Using MSN as the core, silk fibroin protein (ApSF) containing arginine–glycine–aspartate (RGD) tripeptide was utilized for capping.	ICD mediated by phototherapy	Breast cancer	[74]

"–" means no given data in the references.

cell death, while PDT employs photosensitizers to produce ROS, leading to tumor cell necrosis and apoptosis. Due to their non-invasive nature and high selectivity, phototherapy techniques have found wide applications in tumor treatment.

Initially, PTT or PDT was used individually in early research. Subsequently, researchers have preferred their combination [70]. For example, Liu *et al.* loaded DOX with dopamine as a photothermal conversion component and a photosensitizer to design an MNM propelled by thermal

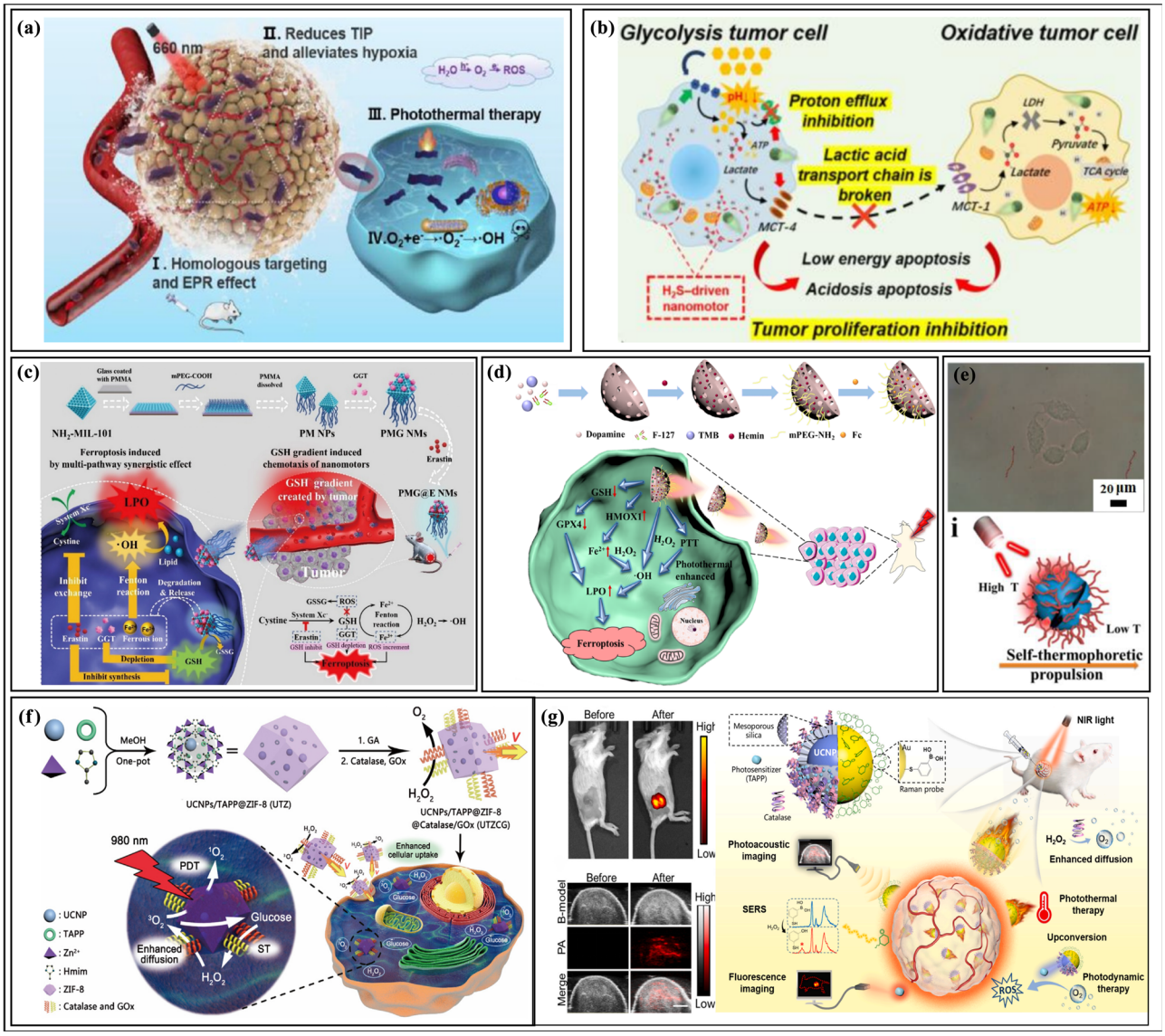

Figure 6: Applications of nanomotors in biomedicine: tumor therapy: (a) illustration of AWS@M for reducing tumor stroma pressure and conducting PTT from the study by Fu *et al.* [63]; (b) schematic diagram depicting the H_2S-driven nanomotor with a payload of α-CHCA, a monocarboxylate transporter inhibitor, for disrupting tumor metabolism from the study by Wan *et al.* [65]; (c) schematic diagram depicting the synthesis of GSH-induced chemotactic PMG NMs and therapeutic mechanism from the study by Qian *et al.* [67]; (d) schematic diagram illustrating the synthesis of NIR-driven PHPF nanomotors in the tumor microenvironment and their photothermal-enhanced motion from the study by Zhang *et al.* [69]; (e) trajectory plot (top) and pattern diagram of walnut-shaped PDA MNMs motion under NIR irradiation (bottom) from the study by Liu *et al.* [71]; (f) schematic diagram of UTZCG nanomotor fabrication and photodynamic-starvation therapy process from the study by You *et al.* [72]; and (g) schematic diagram of dual-driven nanomotors for SERS biosensing and cancer phototherapy (right), *in vivo* fluorescence imaging before and after the injection of UMSTCA3 nanomotors at the tumor site in tumor-bearing mice (top left), and PAI of tumor-bearing mice (bottom-right) from the study by Chen *et al.* [75]. AWS Ag_2S/WS_2, M membrane; α-CHCA: alpha-cyano-4-hydroxycinnamic acid; GSH, glutathione; PMG NMs mPEG@MIL-101@GGT nanomotors, PHPF polydopamine-hemin-PEG-ferrocene; UTZCG UCNPs/TAPP@ZIF-8@Catalase/GOx; SERS: surface-enhanced Raman scattering; UMSTCA3, UCNPs@mSiO2-TAPP/catalase@Au-3-MPBA; PAI: photoacoustic imaging.

gradients (Figure 6e). Upon reaching the lesion site, the drug delivery system releases chemotherapy drugs, synergistically treating tumors through photothermal conversion effects and drug coadministration, termed photothermal chemotherapy [71]. You *et al.* combined PDT with starvation therapy (Figure 6f) by coating upconversion nanoparticles with ZIF-8 to create a core–shell structure for loading PSs, CAT, and GOx to help alleviate tumor hypoxia and glucose consumption in the tumor microenvironment [72]. This approach has been used by Li *et al.* for the treatment of glioblastoma multiforme (GBM) [73]. The ICD effect mediated by phototherapy is also an important pathway in tumor phototherapy. The cytotoxic singlet oxygen ($1O_2$) generated by phototherapy not only directly kills tumor cells but also triggers ICD, influencing the release of TAAs, DAMPs, and cytokines. Zhang *et al.* reported a photoimmunotherapy-based drug delivery platform combined with chemotherapy to jointly eliminate tumor cells [74]. Chen *et al.* devised an integrated platform (Figure 6g) that combines surface-enhanced Raman scattering (SERS) sensing, fluorescence imaging/photoacoustic imaging (PAI), PDT, and PTT. This MNM can detect H_2O_2 signals and has the capability for PAI/FLI bimodal imaging and NIR-triggered PTT/PDT synergistic phototherapy [75].

3.1.3 Biosensing and imaging

MNMs have not only been directly applied in disease treatment but also driven the preparation and investigation of biosensors and biomedical imaging systems [178].

Changes in the active motion behavior of MNMs can be correlated with electrical signals to develop sensor systems. It has been reported by researchers that the Zika virus can impact the catalytic performance of catalytic components such as Pt, specifically the virus concentration. These findings can be utilized for pathogen detection and management [78]. Increasing the detection sensitivity is an ongoing objective for biosensor researchers.

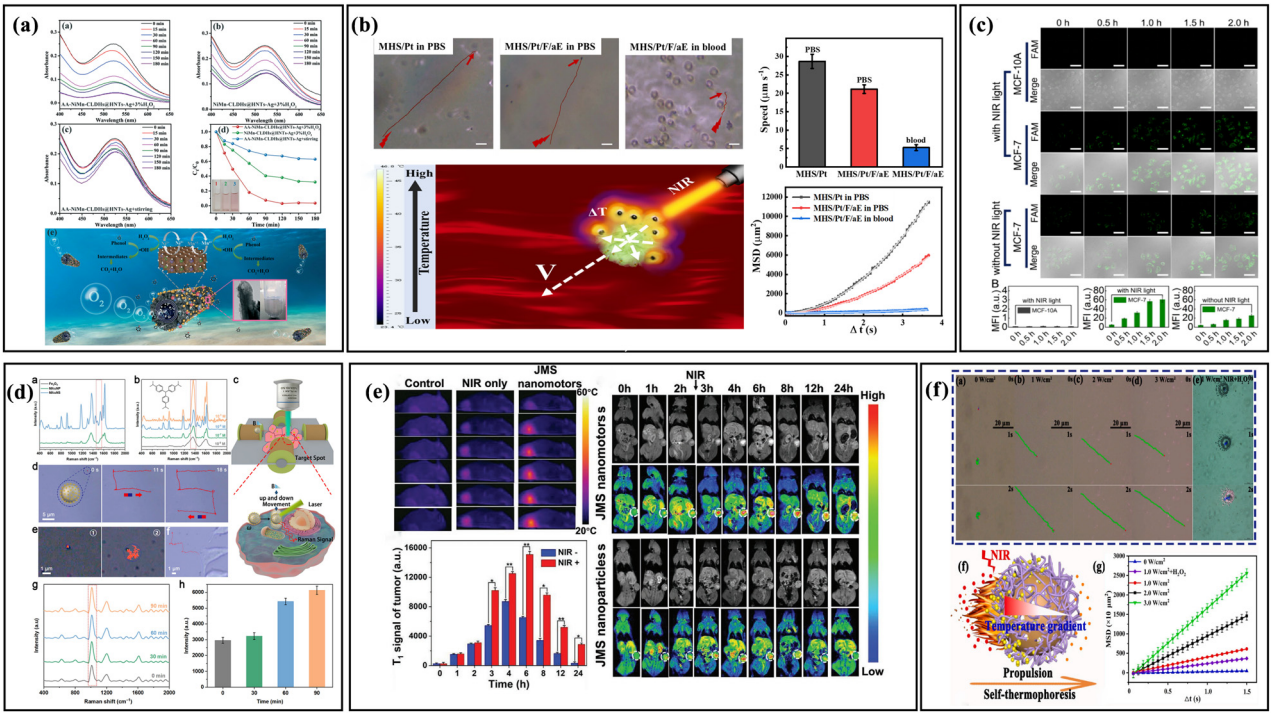

Figure 7: Applications of nanomotors in biomedicine: biosensing and imaging: (a) UV-Vis absorption spectra (top) and degradation mechanism (bottom) schematics of phenol by nanomotors from the study by Wang *et al.* [79]; (b) illustration of trajectory (top-left), potential mechanisms (bottom-left), and quantitative analysis (right) of MHS/Pt nanomotors in PBS and blood from the study by Xu *et al.* [80]; (c) confocal laser scanning microscopic images of miRNA21 in MN-10A and MCF-7 cells at different time points (top); corresponding mean fluorescence intensity images for MCF-10A and MCF-7 cells (bottom) from the study by Lin *et al.* [88]; (d) different Raman spectra obtained using nanorobot probes under various conditions, schematic diagrams of targeted cells, and intracellular SERS signal intensities from the study by Liu *et al.* [83]; (e) *in vivo* MR imaging tests of JMS nanomotors from the study by Zheng *et al.* [85]; (f) time-lapse images of Au/Cu-CeO_2@BSA Janus nanomotors under different NIR light intensities and schematic diagrams illustrating possible motion mechanisms from the study by Zhang *et al.* [87]. MHS: hierarchical silica nanoparticles; JMS: Janus mesoporous silica; BSA: bovine serum albumin.

Capturing target biomolecules is a crucial step in biosensing because it directly affects the performance of biosensors. Researchers are continuously working to enhance capture efficiency by increasing the opportunities for interactions between materials and biomarkers. The use of MNMs with autonomous motion is envisioned to improve the binding probability between nanomaterials and targets in biosensing, thereby enabling more effective biosensor performance. For instance, Xing *et al.* developed a pollutant detection and removal system for phenol detection utilizing ascorbic acid functionalization (Figure 7a). To propel the MNMs, AgNPs were introduced into the lumens of halloysite nanotubes as catalysts for H_2O_2 decomposition, generating O_2 bubbles. The motion of these MNMs enhances solution diffusion, facilitating their interaction with pollutants and resulting in a detection limit of 0.225 μM [79]. Recently, Xu *et al.* prepared magnetic hierarchical silica (MHS) NPs/Pt MNMs (Figure 7b) supplemented with fluorescein isothiocyanate to enable visual detection. These MNMs had an iron oxide (Fe_3O_4) NP core, which was surface-modified with a layered silica shell. Subsequently, Pt NPs were generated by the *in situ* reduction of chloroplatinic acid within the shell. This system is capable of efficiently and safely detecting and capturing circulating tumor cells in unprocessed whole blood while minimizing adverse effects on cells and protein [80]. Lin *et al.* noted that the concentration of miRNA in cells is nanomolar, and highly sensitive detection methods are required for *in situ* imaging analysis of live cells. In this JN@MnO_2@hQN nanoplatform (Figure 7c), gold shells encapsulated on one side of mesoporous silica enable the propulsion of MNMs under NIR irradiation-induced thermal gradients. MnO_2 nanosheets can enhance the ability of the nanoplatform to be taken up by cells to some extent and partially suppress the fluorescence of non-targeted hairpin DNA quadrangular nanostructure(hQN) outside the cells. Once inside the cells, JN@MnO_2@hQN provides more opportunities for hQN to interact with the target miRNA, triggering more sensitive imaging [88].

The inherent autonomous mobility and modifiability of MNMs contribute to enhancing the performance of existing biomedical imaging systems. Previous research has utilized MNMs as a foundation for developing imaging system probes, contrast agents, and biomarker carriers, among other applications. Traditional SERS probes rely on the passive diffusion of analytes or SERS nanoprobes for contact, which is a process with poor controllability. In a study conducted by Wang *et al.*, a "rod-shaped" magnetic nanomotor-based SERS probe (MNM-SP) was proposed. Individual MNM-SPs can accurately approach target locations along predesigned paths and then actively rotate to enhance contact with analytes. Compared to non-rotating SERS probes, additional Raman signals were observed [81]. An increase in the quantity of enriched SERS probes within the detection system and an increase in the probability of contact between analytes and SERS probes can theoretically improve the quality of detection. The targeting and motility capabilities of MNMs enable them to function effectively as probes [82].

Furthermore, Liu *et al.* developed a core-island structured magnetic MNMs, called MAuNS, in which the motion of the MNMs could be controlled by external magnetic field parameters (Figure 7d). The AuNS islands exhibited glucose catalytic activity, facilitating glucose decomposition and propelling the motion of the MNMs toward the target locations. In addition, the AuNS islands served as efficient plasmonic components capable of generating SERS effects, thereby functioning as SERS probes for sensing applications [83].

Moreover, Zhang *et al.* engineered MNMs based on halloysites encapsulating DOX/Au-m-HTAS, demonstrating their ability to enhance computed tomography imaging for diagnostic purposes [84]. Similarly, Zheng *et al.* proposed NIR-propelled JMS MNMs constructed using Gd(III)-doped MSNs and subsequently deposited Au on one side of the silica NPs (Figure 7e). Gd(III), which possesses seven unpaired electrons and a significant magnetic moment, can reduce the relaxation time of nearby protons, thereby facilitating high-resolution T1 magnetic resonance (MR) imaging of tissues. This system is designed for efficient tumor penetration and enhanced *in vivo* MR imaging [85].

In the process of carrying out biomedical tasks, the position and status of MNMs have significant potential application value as informative data [179]. Studies are focused on real-time monitoring of MNMs within the body. Ren *et al.* modified γ-Fe_2O_3 nanorods with folate (FA) and HA carbon dots as targeting ligands to create MNMs (CD@NMs) using the LbL self-assembly technique. Folate-modified CD@NMs suppress the fluorescence of HA carbon dots. When CD@NMs target tumor cells, the receptors on the cell membrane bind to folate and HA, stopping the suppression and allowing the MNMs to image tumor cells [86]. Zhang *et al.* described a novel Janus MNM driven by NIR light, Au/Cu-CeO2@BSA (ACCB Janus NMs), which was used for active PAI and synergistic PTT/CDT (Figure 7f). Due to the favorable diffusion of MNMs within tumors, PAI can clearly show the position and outline of tumors, providing real-time monitoring for the therapeutic process of MNMs [87].

3.2 Environmental restoration

Conventional wastewater treatment technologies are inadequate for treating heavy metal ions and organic

pollutants in wastewater because they are unable to efficiently access contaminants [180].

MNMs have been widely utilized in the development of wastewater treatment technologies due to their low cost, high pollutant removal efficiency, and robust mobility. Previous studies have focused on the photocatalytic degradation of benzyl bromide and methylene blue in water induced by MNMs [89]. Kutorglo *et al.* fabricated polypyrrole NPs, onto which a cascade of enzymes (GOx and CAT) was unevenly grafted. This innovative approach results in a nanorobotic system that can utilize glucose as fuel to induce the degradation of sulfur-containing pollutants under light irradiation [102]. Most existing wastewater treatment methods are ineffective at removing antibiotic residues. To address this issue, Liu *et al.* developed a light-driven Au–ZnO MNM that enhances the photocatalytic degradation of antibiotics. By utilizing a hydrothermal method to synthesize a ZnO nanorod array, which is then coated with a sputtered Au layer, electron transfer occurs in the ZnO and Au layers under UV light irradiation, leading to water decomposition and self-electrophoretic motion [90]. More recently, Li *et al.* modified the surface of manganese dioxide nanosheets with PDA to create bowl-shaped PDA@MnO_2 MNMs. This MNM combines the catalytic decomposition of H_2O_2 by manganese dioxide nanosheets and the generation of thermal gradients by PDA, resulting in significantly enhanced propulsion capabilities. The actively propelled MNM, which acts as a nanoadsorbent for wastewater, has demonstrated effective removal of various pollutants [91]. Additionally, lead ions are prevalent heavy metal pollutants in water that can cause irreversible damage to the nervous system, especially in children. Pan *et al.* immobilized iron phthalocyanine on mesoporous silica as a photothermal conversion component. By leveraging the ability of mesoporous silica-based materials to adsorb metal ions, MNMs can be used to rapidly separate Pb^{2+} ions from wastewater at a maximum rate of 26 μm/s [92].

4 Summary and outlook

In this review, we summarize the latest advancements in the construction and application of MNMs and categorize these developments. MNMs have been utilized in various biomedical fields, with their active motility and targeting capabilities revolutionizing *in vivo* delivery technologies. This transformation has significantly enhanced delivery efficiency and reduced off-target effects. Various therapeutic approaches, such as physical therapy, biological therapy, chemical drug therapy, and immunotherapy, are continuously being developed and implemented. Furthermore, biosensing technologies derived from MNMs have enhanced detection sensitivity and quality. The potential for removing toxic substances from biological systems may also develop in the future. In addition, researchers are integrating MNMs as probes and imaging agents into traditional medical devices, which demonstrates their vast potential. We anticipate the development of multifunctional MNMs tailored to specific application needs, with various propulsion modes being employed.

However, the development of MNMs encounters numerous challenges. Nevertheless, these challenges can be addressed through further research and expansion of the field.

1) The biosafety and biocompatibility of MNMs, as exogenous components, warrant significant attention. Introducing metal and non-metal compounds into the body may have adverse effects or be cleared by the defensive immune system [181,182]. The safety of biohybrid MNMs is particularly concerning. For instance, MNMs using viruses as carriers may undergo mutations or reactivation, which necessitates stringent inactivation or removal of toxic genes [183]. Similarly, MNMs constructed from bacteria pose potential risks of inducing immune responses or interacting with the *in vivo* microenvironment, which potentially harms the host [184].

   Recent studies have mainly focused on the immediate impact of MNMs on macroscopic biosafety. These works often overlook the cumulative effects and potential toxicity of MNMs within the body. For example, a malfunction of MNMs carrying thrombin could lead to thrombin leakage and abnormal accumulation at critical sites, which potentially trigger thrombosis and endanger patient lives [185]. MNMs left in the body may also induce hypersensitivity reactions and inflammatory damage.

   Ideally, MNMs should remain stable and maintain functional integrity before executing their tasks. They should rapidly degrade into harmless components for excretion after task completion. The development and use of novel biocompatible materials for constructing MNMs, such as polylactic acid, hydrogels, bioglass, graphene and its derivatives, and MOFs, should be explored to enhance their safety and biocompatibility. Improving biocompatibility can also be accomplished by utilizing more biomaterials, including purified serum proteins, cell membranes, signaling molecules, and nucleic acids. Adjusting the size of MNMs to prevent them from accumulating in the body and inducing immune responses is another solution.
2) The fabrication of MNMs is complex and costly. These factors present challenges in storage and stability. The need for personalized customization for different

diseases further diminishes their scalability.

The design and development of new manufacturing processes for MNM structures are crucial for advancing this field. Researchers have started to explore innovative techniques for fabricating MNMs, such as LbL self-assembly [186], colloidal-scale assemblies [187], DNA origami [156], magnetron sputtering [188], 3D printing [189], wafer-scale fabrication [190], and low-temperature shadow deposition [191].

Future research may focus on developing methods for the mass production and industrial-scale fabrication of nanorobots to enhance their stability and versatility. Increased investment in the development of new technologies beyond conventional fabrication methods is necessary to achieve higher energy conversion efficiencies and effective payload capacities.

3) The overall targeting of MNMs remains uncontrollable, and quantitative assessment metrics for the accuracy of different propulsion methods need to be developed to reduce the occurrence of off-target effects. Chemotactic targeting is susceptible to environmental influences and lacks specificity. The local concentration gradients of substances within the body can easily disrupt the directional movement of MNMs. External field targeting can only achieve approximate targeting and is constrained by the range of the external field, with most studies focusing on localized effects. This imprecise targeting leads to a biodistribution of MNMs that is insufficiently concentrated in the intended operational area, which not only reduces their efficacy but also poses potential biological risks. For instance, gas leaks under CO-driven conditions may result in toxicity risks [96].

   Independent design and research of targeting modules through structural design, along with the selection of advanced material substrates, can improve the targeting capabilities of the system. Future research should explore the integration of various biomolecular signals, such as antibodies, nanobodies, phages, nucleic acid aptamers, peptides, and polysaccharides, to enhance the specificity of targeting within biological systems. Additionally, employing multi-modal guidance for targeting, such as enhancing chemotactic MNMs with external physical field assistance, is a valuable approach for improving targeting precision. Incorporating signal amplification mechanisms, such as fluorescent labeling or nanoenzyme reactions, could further increase sensitivity, enabling MNMs to detect target molecules even at low concentrations with greater efficiency.

4) The development of new propulsion methods should focus on obtaining a deep understanding of the underlying mechanisms and elucidating the principles of propulsion. For instance, Gibbs and Zhao achieved complex mechanical movements with self-organizing catalytic MNMs, which are composed of multiple individual components [192]. Similarly, McNeill *et al.* designed MNMs with unique morphologies that can be resonantly propelled under ultrasonic stimulation [190]. Xu *et al.* demonstrated a chemical thermal gradient-driven propulsion, which provided researchers with an alternative to the commonly used photothermal gradient propulsion methods [193].

   Further exploration is required to integrate different propulsion methods. For example, combining chemical propulsion and magnetic propulsion could enhance environmental adaptability and targeting precision. In addition, acoustic–optical cooperative driving may offer deep responsiveness and flexibility. The combination of traditional propulsion methods could yield superior performance and produce unexpected effects.

5) Proposed research directions include integrating multifunctionality and ensuring mutual adaptation between structure and function. Some studies have already designed systems that utilize material and structural properties to enable therapeutic effects while simultaneously providing imaging of the affected areas [30,194]. Bai developed a multifunctional system for treating and managing periodontal disease. This system creates a favorable environment for subsequent periodontal regeneration [195].

   Establishing a multifunctional therapeutic platform, with structural design driven by specific needs, has been proposed. Using the characteristics of materials or structures themselves, the design of drivers, targets, and functions can be modularized. The design of interchangeable functional and power modules enables the reconfiguration and combination of MNMs depending on specific requirements. The incorporation of smart materials, such as polymers or shape memory alloys, endows these nanorobots with self-healing capabilities. In addition, employing multiple power sources allows for autonomous movement in diverse environments, which enhances adaptability. Incorporating various sensor designs, such as temperature-responsive and pH-responsive sensors, can enable real-time responses of MNMs to environmental changes. The abovementioned ideas may all be realized in future research on multifunctional MNMs.

6) MNMs, as a medical device, face complex ethical, moral, and legal issues. The impact of the fabrication and application of MNMs on biological systems lacks real-time and effective regulatory measures, which results in widespread regulatory obstacles. Furthermore, the effects of MNMs upon entering biological organisms have not been thoroughly investigated. This lack makes their

long-term safety unconvincing. Regulatory authorities and researchers should enhance the technical and ethical oversight of MNMs, refine existing laws, and conduct further research throughout the entire application process to ensure their transition into clinical practice.

We believe that precision medical technologies based on MNMs hold promise for safer and more effective practical applications. The thriving fields of nanomaterials and fundamental medicine will continue to drive the strong momentum of MNMs research.

Funding information: This study was supported by grants from the National Natural Science Foundation of China (NSFC#82370701).

Author contributions: Kun Yuan: conceptualization, investigation, methodology, project administration, validation, visualization, writing – original draft, writing – review and editing. Danting Shu: conceptualization, investigation, methodology, validation, writing – original draft, writing – review and editing. Xing Li: funding acquisition, supervision, writing – review and editing. Zihao Guo: investigation, methodology, validation, writing – original draft, writing – review and editing. Xiang Ren: visualization, methodology, writing – review and editing. Yiqun Tian: investigation, writing – original draft, writing – review and editing. Zhenliang Tan: investigation. Zhixian Wang: supervision, investigation. Jing Wang: validation, writing – original draft, writing – review and editing. Yisheng Yin: validation, writing – original draft, writing – review and editing. Xiaoyong Zeng: conceptualization, funding acquisition, methodology, project administration, supervision, validation, visualization, writing – original draft, writing – review and editing. All authors have accepted responsibility for the entire content of this manuscript and approved its submission.

Conflict of interest: The authors state no conflict of interest.

Data availability statement: All data generated or analyzed during this study are included in this published article.

References

[1] Sheth V, Wang L, Bhattacharya R, Mukherjee P, Wilhelm S. Strategies for delivering nanoparticles across tumor blood vessels. Adv Funct Mater. 2020;31(8).

[2] Luo M, Feng Y, Wang T, Guan J. Micro-/nanorobots at work in active. Drug Deliv. 2018;28.

[3] Mitchell MJ, Billingsley MM, Haley RM, Wechsler ME, Langer R. Engineering precision nanoparticles for drug delivery. Nat Rev Drug Discov. 2020;20(2):101–24.

[4] Chen Q, Yang Z, Liu H, Man J, Oladejo AO, Ibrahim S, et al. Novel drug delivery systems: an important direction for drug innovation research and development. Pharmaceutics. 2024;16:674.

[5] Chen D, Cai L, Guo Y, Chen J, Gao Q, Yang J, et al. Cancer cell membrane-decorated zeolitic-imidazolate frameworks codelivering cisplatin and oleanolic acid induce apoptosis and reversed multidrug resistance on bladder carcinoma cells. ACS Omega. 2020;5(2):995–1002.

[6] Lu M, Huang Y. Bioinspired exosome-like therapeutics and delivery nanoplatforms. Biomaterials. 2020;242:119925.

[7] Adepu S, Ramakrishna S. Controlled drug delivery systems: current status and future directions. Molecules. 2021;26(19):5905.

[8] Vale RD, Milligan RA. The way things move: looking under the hood of molecular motor proteins. Science. 2000;288(5463):88–95.

[9] Ismagilov RF, Schwartz A, Bowden N, Whitesides GM. Autonomous movement and self-assembly. Angew Chem Int Ed. 2002;41(4):652–4.

[10] Kline TR, Paxton WF, Mallouk TE, Sen A. Catalytic nanomotors: remote-controlled autonomous movement of striped metallic nanorods. Angew Chem Int Ed. 2005;44(5):744–6.

[11] Paxton WF, Sen A, Mallouk TEJC. Motility of catalytic nanoparticles through self-generated forces. ChemInform. 2006;11:6462–70.

[12] Zhou H, Yuan Y, Wang Z, Ren Z, Hu M, Lu J, et al. Co-delivery of doxorubicin and quercetin by Janus hollow silica nanomotors for overcoming multidrug resistance in breast MCF-7/Adr cells. Colloids Surf A. 2023;658:130654.

[13] Luo Z, Wang R, Deng X, Chen T, Ma X, Zhang Y, et al. Janus mesoporous organosilica/platinum nanomotors for active treatment of suppurative otitis media. Nanoscale. 2024;16(6):3006–10.

[14] Wang H, Chen X, Qi Y, Wang C, Huang L, Wang R, et al. Self-propelled nanomotors with an alloyed engine for emergency rescue of traumatic brain injury. Adv Mater. 2022;34(49):e2206779.

[15] Yu J, Li Y, Yan A, Gao Y, Xiao F, Xu Z, et al. Self-propelled enzymatic nanomotors from prodrug-skeletal zeolitic imidazolate frameworks for boosting multimodel cancer therapy efficiency. Adv Sci. 2023;10(22):e2301919.

[16] Chang CW, Gong ZJ, Huang NC, Wang CY, Yu WY. Water powered and anti-CD3 loaded mg micromotor for t cell activation. Appl Mater Today. 2020;351:21–9.

[17] Zhang J, Zhang K, Hao Y, Yang H, Wang J, Zhang Y, et al. Polydopamine nanomotors loaded indocyanine green and ferric ion for photothermal and photodynamic synergistic therapy of tumor. J Colloid Interface Sci. 2022;633:679–90.

[18] Ji Y, Pan Y, Ma X, Ma Y, Zhao Z, He Q. pH-sensitive glucose-powered nanomotors for enhanced intracellular drug delivery and ferroptosis efficiency. Chem – Asian J. 2023;19(1):e202300879.

[19] Ma X, Jannasch A, Albrecht UR, Hahn K, Miguel-López A, Schäffer E, et al. Enzyme-powered hollow mesoporous janus nanomotors. Nano Lett. 2015;15(10):7043–50.

[20] Yang Z, Wang L, Gao Z, Hao X, Luo M, Yu Z, et al. Ultrasmall enzyme-powered janus nanomotor working in blood circulation system. ACS Nano. 2023;17(6):6023–35.

[21] Llopis-Lorente A, García-Fernández A, Murillo-Cremaes N, Hortelão AC, Patiño T, Villalonga R, et al. Enzyme-powered gated

mesoporous silica nanomotors for on-command intracellular payload delivery. ACS Nano. 2019;13(10):12171–83.
[22] Feng Y, Yuan Y, Wan J, Yang C, Hao X, Gao Z, et al. Self-adaptive enzyme-powered micromotors with switchable propulsion mechanism and motion directionality. Appl Phys Rev. 2021;8(1):011406.
[23] Kaang BK, Ha L, Joo J-U, Kim D-P. Laminar flow-assisted synthesis of amorphous ZIF-8-based nano-motor with enhanced transmigration for photothermal cancer therapy. Nanoscale. 2022;14(30):10835–43.
[24] Cao Y, Liu S, Ma Y, Ma L, Zu M, Sun J, et al. Oral nanomotor-enabled mucus traverse and tumor penetration for targeted chemo-sono-immunotherapy against colon cancer. Small. 2022;18(42):2203466.
[25] Wang W, Castro LA, Hoyos M, Mallouk TE. Autonomous motion of metallic microrods propelled by ultrasound. ACS Nano. 2012;6(7):6122–32.
[26] Yu X, Li X, Chen Q, Wang S, Xu R, He Y, et al. High intensity focused ultrasound-driven nanomotor for effective ferroptosis-immunotherapy of TNBC. Adv Sci. 2024;11:e2305546.
[27] Zhang F, Zhuang J, Esteban Fernández de Ávila B, Tang S, Zhang Q, Fang RH, et al. A nanomotor-based active delivery system for intracellular oxygen transport. ACS Nano. 2019;13(10):11996–2005.
[28] Bhuyan T, Dutta D, Bhattacharjee M, Singh AK, Ghosh SS, Bandyopadhyay D. Acoustic propulsion of vitamin c loaded teabots for targeted oxidative stress and amyloid therapeutics. ACS Appl Bio Mater. 2019;2(10):4571–82.
[29] Ye J. Ultrasound-propelled Janus Au NR-mSiO_2 nanomotor for NIR-II photoacoustic imaging guided sonodynamic-gas therapy of large tumors. Sci China Chem. 2021;64:2218–29.
[30] Feng J, Yang SP, Shao YQ, Sun YY, He ZL, Wang Y, et al. Covalent organic framework-based nanomotor for multimodal cancer photo-theranostics. Adv Healthc Mater. 2023;12(30):2301645.
[31] Hong Y, Diaz M, Córdova-Figueroa UM, Sen A. Light-driven titanium-dioxide-based reversible microfireworks and micromotor/micropump systems. Adv Funct Mater. 2010;20(10):1568–76.
[32] Cui D, Lyu X, Duan S, Peng Y, Wang W. Rhodium oxide nanorod motors powered by light across the full visible spectrum. ACS Appl Nano Mater. 2022;5(10):14235–40.
[33] Wang D, Jiang J, Hao B, Li M, Chen Z, Zhang H, et al. Bio-inspired micro/nanomotor with visible light dependent in situ rotation and phototaxis. Appl Mater Today. 2022;29:101652.
[34] Mou F, Li Y, Chen C, Li W, Yin Y, Ma H, et al. Single-component TiO_2 tubular microengines with motion controlled by light-induced bubbles. Small. 2015;11(21):2564–70.
[35] Kausar A, Nagano H, Ogata T. Photocontrolled translational motion of a microscale solid object on azobenzene-doped liquid-crystalline films. Environ Monit Assess. 2008;157:347–54.
[36] Liu W, Wang W, Dong X, Sun Y. Near-infrared light-powered janus nanomotor significantly facilitates inhibition of amyloid-β fibrillogenesis. ACS Appl Mater Interfaces. 2020;12(11):12618–28.
[37] Gui L, Huang J, Xing Y, Li Y, Zou J, Zhu Y, et al. Near-infrared light-driven multifunctional metal ion (Cu2 +)-loaded polydopamine nanomotors for therapeutic angiogenesis in critical limb ischemia. Nano Res. 2023;16(4):5108–20.
[38] Ji X, Yang H, Liu W, Ma Y, Wu J, Zong X, et al. Multifunctional parachute-like nanomotors for enhanced skin penetration and synergistic antifungal therapy. ACS Nano. 2021;15(9):14218–28.
[39] Zhang Z, Yan H, Cao W, Xie S, Ran P, Wei K, et al. Ultrasound-chargeable persistent luminescence nanoparticles to generate self-propelled motion and photothermal/NO therapy for synergistic tumor treatment. ACS Nano. 2023;17(16):16089–106.
[40] Calvo-Marzal P, Sattayasamitsathit S, Balasubramanian S, Windmiller JR, Dao C, Wang J. Propulsion of nanowire diodes. Chem Commun. 2010;46(10):1623–4.
[41] Ayranci R, Celik Cogal G, Ak M, Uygun Oksuz A. A novel type of multifunctional pRM@Au-Ni micromotor for screening of Hg^{2+} heavy metal ion. Microchem J. 2023;193:109166.
[42] Gao W, Kagan D, Pak OS, Clawson C, Campuzano S, Chuluun-Erdene E, et al. Cargo-towing fuel-free magnetic nanoswimmers for targeted drug delivery. Small. 2011;8(3):460–7.
[43] Feng Z-Q, Yan K, Li J, Xu X, Yuan T, Wang T, et al. Magnetic Janus particles as a multifunctional drug delivery system for paclitaxel in efficient cancer treatment. Mater Sci Eng C. 2019;104:104.
[44] Sun Y, Pan R, Chen Y, Wang Y, Sun L, Wang N, et al. Efficient preparation of a magnetic helical carbon nanomotor for targeted anticancer drug delivery. ACS Nanosci Au. 2022;3(1):94–102.
[45] Wang M, Bao T, Yan W, Fang D, Yu Y, Liu Z, et al. Nanomotor-based adsorbent for blood Lead(II) removal in vitro and in pig models. Bioact Mater. 2021;6(4):1140–9.
[46] Byun J-K. Tumor lactic acid: a potential target for cancer therapy. Arch Pharmacal Res. 2023;46(2):90–110.
[47] Liu M, Pan L, Piao H, Sun H, Huang X, Peng C, et al. Magnetically actuated wormlike nanomotors for controlled cargo release. ACS Appl Mater Interfaces. 2015;7(47):26017–21.
[48] Dreyfus R, Baudry J, Roper ML, Fermigier M, Stone HA, Bibette J. Microscopic artificial swimmers. Nature. 2005;437(7060):862–5.
[49] Li T, Liu Z, Hu J, Chen L, Chen T, Tang Q, et al. A universal chemotactic targeted delivery strategy for inflammatory diseases. Adv Mater. 2022;34(47):2206654.
[50] Wang H, Gao J, Xu C, Jiang Y, Liu M, Qin H, et al. Light-driven biomimetic nanomotors for enhanced photothermal therapy. Small. 2023;20(3):e2306208.
[51] Wang Q, Zhou R, Sun J, Liu J, Zhu Q. Naturally derived janus cellulose nanomaterials: anisotropic cellulose nanomaterial building blocks and their assembly into asymmetric structures. ACS Nano. 2022;16(9):13468–91.
[52] Xu X, Huo Z, Guo J, Liu H, Qi X, Wu Z. Micromotor-derived composites for biomedicine delivery and other related purposes. Bio-Des Manuf. 2020;3(2):133–47.
[53] Głowienke H, Livraghi S, Lisowski W, Klimczuk T, Mikolajczyk A, Falkowski D, et al. From Janus nanoparticles to multi-headed structure - photocatalytic H_2 evolution. Int J Hydrog Energy. 2024;59:808–24.
[54] Medina-Sánchez M, Xu H, Schmidt OG. Micro- and nano-motors: the new generation of drug carriers. Ther Deliv. 2018;9(4):303–16.
[55] Wan M, Wang Q, Wang R, Wu R, Li T, Fang D, et al. Platelet-derived porous nanomotor for thrombus therapy. Sci Adv. 2020;6(22):eaaz9014.
[56] Choi H, Cho SH, Hahn SK. Urease-powered polydopamine nanomotors for intravesical therapy of bladder diseases. ACS Nano. 2020;14(6):6683–92.
[57] Ma Y, Gou S, Zhu Z, Sun J, Shahbazi MA, Si T, et al. Transient mild photothermia improves therapeutic performance of oral nanomedicines with enhanced accumulation in the colitis mucosa. Adv Mater. 2024;36:e2309516.
[58] Cheng G, Han X, Zheng S-Y. Magnetically driven nanotransporter-assisted intracellular delivery and autonomous release of proteins. ACS Appl Mater Interfaces. 2020;12(37):41096–104.

[59] Meng J, Wei K, Xie S, Zhang Z, Ran P, Zhang P, et al. Pyroelectric Janus nanomotors to promote cell internalization and synergistic tumor therapy. J Control Release. 2023;357:342–55.
[60] Meng J, Zhang P, Liu Q, Ran P, Xie S, Wei J, et al. Pyroelectric Janus nanomotors for synergistic electrodynamic-photothermal-antibiotic therapies of bacterial infections. Acta Biomater. 2023;162:20–31.
[61] Zhao Y, Liu Y, Liao R, Ran P, Liu Y, Li Z, et al. Biofilm microenvironment-sensitive piezoelectric nanomotors for enhanced penetration and ROS/NO synergistic bacterial elimination. ACS Appl Mater Interfaces. 2024;16(3):3147–61.
[62] Wu Z, Troll J, Jeong HH, Wei Q, Stang M, Ziemssen F, et al. A swarm of slippery micropropellers penetrates the vitreous body of the eye. Sci Adv. 2018;4(11):eaat4388.
[63] Fu Y, Ye F, Zhang X, He Y, Li X, Tang Y, et al. Decrease in tumor interstitial pressure for enhanced drug intratumoral delivery and synergistic tumor therapy. ACS Nano. 2022;16:18376–89.
[64] Zhang Z, Zhong H, Zhou Y, Ke P, Dai Q, Lu Y, et al. Lactate-driving Pt nanoflower with positive chemotaxis for deep intratumoral penetration. Nano Today. 2022;45:101542.
[65] Wan M, Liu Z, Li T, Chen H, Wang Q, Chen T, et al. Zwitterion-based hydrogen sulfide nanomotors induce multiple acidosis in tumor cells by destroying tumor metabolic symbiosis. Angew Chem Int Ed. 2021;60(29):16139–48.
[66] Wang Y, Chen W, Wang Z, Zhu Y, Zhao H, Wu K, et al. NIR-II light powered asymmetric hydrogel nanomotors for enhanced immunochemotherapy. Angew Chem Int Ed. 2022;62(3):202212866.
[67] Qian J, Xu Z, Meng C, Liu Y, Wu H, Wang Y, et al. GSH-induced chemotaxis nanomotors for cancer treatment by ferroptosis strategy. Sci China Chem. 2022;65(5):14.
[68] Ou J, Tian H, Wu J, Gao J, Jiang J, Liu K, et al. MnO_2-based nanomotors with active fenton-like Mn^{2+} delivery for enhanced chemodynamic therapy. ACS Appl Mater Interfaces. 2021;13:38050–60.
[69] Zhang Y, Zhang K, Yang H, Hao Y, Zhang J, Zhao W, et al. Highly penetrable drug-loaded nanomotors for photothermal-enhanced ferroptosis treatment of tumor. ACS Appl Mater Interfaces. 2023;15:14099–110.
[70] Xian T, Liu Y, Song Q, Li J, Liu W, Gu Z. NIR-Mediated Cu_2O/Au nanomotors for synergistically treating hepatoma carcinoma cells. Chem – Asian J. 2024;19:e202301137.
[71] Liu Y, Zhang Y, Wang J, Yang H, Zhou J, Zhao W. Doxorubicin-Loaded walnut-shaped polydopamine nanomotor for photothermal-chemotherapy of cancer. Bioconjugate Chem. 2022;33:726–35.
[72] You Y, Xu D, Pan X, Ma X. Self-propelled enzymatic nanomotors for enhancing synergetic photodynamic and starvation therapy by self-accelerated cascade reactions. Appl Mater Today. 2019;16:508–17.
[73] Li T, Chen L, Xue Y, Xiao X, Dai W, Tan K, et al. Chemotactic nanomotor for multimodal combined therapy of glioblastoma. Sci China Chem. 2024;67:1277–88.
[74] Zhang X, He Q, Sun J, Gong H, Cao Y, Duan L, et al. Near-infrared-enpowered nanomotor-mediated targeted chemotherapy and mitochondrial phototherapy to boost systematic antitumor immunity. Adv Healthc Mater. 2022;11(14):2200255.
[75] Chen S, Sun X, Fu M, Liu X, Pang S, You Y, et al. Dual-source powered nanomotor with integrated functions for cancer photo-theranostics. Biomaterials. 2022;288:121744.
[76] Beltrán-Gastélum M, Esteban-Fernández de Ávila B, Gong H, Venugopalan PL, Hianik T, Wang J, et al. Rapid detection of AIB1 in breast cancer cells based on aptamer-functionalized nanomotors. ChemPhysChem. 2019;20(23):3177–80.
[77] Ruan R, Chen S, Su J, Liu N, Feng H, Xiao P, et al. Targeting nanomotor with near-infrared/ultrasound triggered-transformation for polystage-propelled cascade thrombolysis and multimodal imaging diagnosis. Adv Healthc Mater. 2023;13(5):2302591.
[78] Draz MS, Lakshminaraasimulu NK, Krishnakumar S, Battalapalli D, Vasan A, Kanakasabapathy MK, et al. Motion-based immunological detection of zika virus using Pt-nanomotors and a cellphone. ACS Nano. 2018;12(6):5709–18.
[79] Xing N, Lyu Y, Yang J, Zhang X, Han Y, Zhao W, et al. Motion-based phenol detection and degradation using 3D hierarchical AA-NiMn-CLDHs@HNTs-Ag nanomotors. Environ Sci. 2022;9(8):2815–26.
[80] Xu P, Yu Y, Li T, Chen H, Wang Q, Wang M, et al. Near-infrared-driven fluorescent nanomotors for detection of circulating tumor cells in whole blood. Anal Chim Acta. 2020;1129:60–8.
[81] Wang Y, Liu Y, Li Y, Xu D, Pan X, Chen Y, et al. Magnetic Nanomotor-based maneuverable SERS probe. Research. 2020;2020:7962024.
[82] Wang Y, Zhou C, Wang W, Xu D, Zeng F, Zhan C, et al. Photocatalytically powered matchlike nanomotor for light-guided active SERS sensing. Angew Chem Int Ed. 2018;57(40):13110–3.
[83] Liu S, Xu D, Chen J, Peng N, Ma T, Liang F. Nanozymatic magnetic nanomotors for enhancing photothermal therapy and targeting intracellular SERS sensing. Nanoscale. 2023;15(31):12944–53.
[84] Zhang X, Wang Z, Lyu Y, Li J, Song K, Xing N, et al. NIR light-powered halloysite-based nanomotors for CT imaging diagnosis and synergistic chemo-photothermal cancer therapy. J Ind Eng Chem. 2022;116:180–90.
[85] Zheng S, Wang Y, Pan S, Ma E, Jin S, Jiao M, et al. Biocompatible nanomotors as active diagnostic imaging agents for enhanced magnetic resonance imaging of tumor tissues in vivo. Adv Funct Mater. 2021;31(24):2100936.
[86] Ren J, Chen Z, Ma E, Wang W, Zheng S, Wang H. Dual-source powered nanomotors coupled with dual-targeting ligands for efficient capture and detection of CTCs in whole blood and in vivo tumor imaging. Colloids Surf, B. 2023;231:231.
[87] Zhang X, Liu C, Lyu Y, Xing N, Li J, Song K, et al. NIR-propelled Janus nanomotors for active photoacoustic imaging and synergistic photothermal/chemodynamic therapy. J Colloid Interface Sci. 2023;648:457–72.
[88] Lin F, Shao Y, Wu Y, Zhang Y. NIR light-propelled janus-based nanoplatform for cytosolic-fueled microRNA imaging. ACS Appl Mater Interfaces. 2021;13(3):3713–21.
[89] Mallick A, Roy S. Visible light driven catalytic gold decorated soft-oxometalate (SOM) based nanomotors for organic pollutant remediation. Nanoscale. 2018;10(26):12713–22.
[90] Liu M, Jiang J, Tan H, Chen B, Ou J, Wang H, et al. Light-driven Au–ZnO nanorod motors for enhanced photocatalytic degradation of tetracycline. Nanoscale. 2022;14(35):12804–13.
[91] Li X, Zhao Y, Wang D, Du X. Dual-propelled PDA@MnO_2 nanomotors with NIR light and H2O2 for effective removal of heavy metal and organic dye. Colloids Surf A. 2023;658:658.
[92] Pan K, Tang X, Qu G, Tang H, Wei K, Lv J. Mesoporous silica/iron phthalocyanine light-driven nanomaterials for efficient removal of Pb^{2+} Ions from Wastewater. ACS Appl Nano Mater. 2023;6(14):12816–27.

[93] Li H, Peng F, Yan X, Mao C, Ma X, Wilson DA, et al. Medical micro- and nanomotors in the body. Acta Pharma Sin B. 2023;13(2):517–41.
[94] Yong J, Mellick AS, Whitelock J, Wang J, Liang K. A biomolecular toolbox for precision nanomotors. Adv Mater. 2023;35(15):e2205746.
[95] Sundararajan S, Lammert PE, Zudans AW, Crespi VH, Sen A. Catalytic motors for transport of colloidal cargo. Nano Lett. 2008;8(5):1271–6.
[96] Tong F, Liu J, Zhong Y, Xue Y, Luo L, Wang Z, et al. Carbon monoxide-propelled nanomotors as an active treatment for renal injury. Appl Mater Today. 2023;32:32.
[97] Chen T, Duan Y, Dai W, Guo W, Jing P, Ma S, et al. Carbon monoxide-releasing nanomotors based on endogenous biochemical reactions for tumor therapy. J Colloid Interface Sci. 2024;663:396–404.
[98] Tong F, Liu J, Luo L, Qiao L, Wu J, Wu G, et al. pH/ROS-responsive propelled nanomotors for the active treatment of renal injury. Nanoscale. 2023;15(14):6745–58.
[99] Zhao Z, Chen L, Yang C, Guo W, Huang Y, Wang W, et al. Nanomotor-based H_2S donor with mitochondrial targeting function for treatment of Parkinson's disease. Bioact Mater. 2024;31:578–89.
[100] Sun S, Li Z, Ren Z, Li Y. Enzyme-powered nanomotors with enhanced cell uptake and lysosomal escape for combined therapy of cancer. Appl Mater Today. 2022;27:101445.
[101] Guo Z, Liu J, Li Y, McDonald JA, Bin Zulkifli MY, Khan SJ, et al. Biocatalytic metal–organic framework nanomotors for active water decontamination. Chem Commun. 2020;56(94):14837–40.
[102] Yu W, Lin R, He X, Yang X, Zhang H, Hu C, et al. Self-propelled nanomotor reconstructs tumor microenvironment through synergistic hypoxia alleviation and glycolysis inhibition for promoted anti-metastasis. Acta Pharm Sin B. 2021;11(9):2924–36.
[103] Dhar P, Narendren S, Gaur SS, Sharma S, Kumar A, Katiyar V. Self-propelled cellulose nanocrystal based catalytic nanomotors for targeted hyperthermia and pollutant remediation applications. Int J Biol Macromol. 2020;158:1020–36.
[104] Zhang H, Cao Z, Zhang Q, Xu J, Yun SLJ, Liang K, et al. Chemotaxis-driven 2D nanosheet for directional drug delivery toward the tumor microenvironment. Small. 2020;16(44):2002732.
[105] Zheng J, Wang W, Gao X, Zhao S, Chen W, Li J, et al. Cascade catalytically released nitric oxide-driven nanomotor with enhanced penetration for antibiofilm. Small. 2022;18(52):2205252.
[106] Tao Y, Li X, Wu Z, Chen C, Tan K, Wan M, et al. Nitric oxide-driven nanomotors with bowl-shaped mesoporous silica for targeted thrombolysis. J Colloid Interface Sci. 2022;611:61–70.
[107] Chen H, Shi T, Wang Y, Liu Z, Liu F, Zhang H, et al. Deep penetration of nanolevel drugs and micrometer-level t cells promoted by nanomotors for cancer immunochemotherapy. J Am Chem Soc. 2021;143(31):12025–37.
[108] Zhou C, Zhang HP, Tang J, Wang W. Photochemically powered AgCl janus micromotors as a model system to understand ionic self-diffusiophoresis. Langmuir. 2018;34(10):3289–95.
[109] Rosli NF, Mayorga-Martinez CC, Fisher AC, Alduhaish O, Webster RD, Pumera M. Arsenene nanomotors as anticancer drug carrier. Appl Mater Today. 2020;21:100819.
[110] Liu R, Sen A. Autonomous nanomotor based on copper–platinum segmented nanobattery. J Am Chem Soc. 2011;133(50):20064–7.
[111] Gao W, Sattayasamitsathit S, Uygun A, Pei A, Ponedal A, Wang JJN. Polymer-based tubular microbots: role of composition and preparation. Nanoscale. 2012;4(7):2447–53.
[112] Song ZL, Zhao L, Ma T, Osama A, Shen T, He Y, et al. Progress and perspective on hydrogen sulfide donors and their biomedical applications. Med Res Rev. 2022;42(5):1930–77.
[113] Gao W, Uygun A, Wang J. Hydrogen-bubble-propelled zinc-based microrockets in strongly acidic media. J Am Chem Soc. 2012;134(2):897–900.
[114] Duan H, Heng L, Ou X, Zhang H, Guo H, Fan L, et al. Magnesium-coated hydroxyapatite/titania cement as a potential nanomotor-based coating on orthopedic implant. Mater Lett. 2022;316:132042.
[115] Wang Y, Hernandez RM, Bartlett DJ Jr, Bingham JM, Kline TR, Sen A, et al. Bipolar electrochemical mechanism for the propulsion of catalytic nanomotors in hydrogen peroxide solutions. Langmuir. 2006;22(25):10451–6.
[116] Gaspard P, Kapral R. Thermodynamics and statistical mechanics of chemically powered synthetic nanomotors. Adv Phys: X. 2019;4(1):1602480.
[117] Kuron M, Kreissl P, Holm C. Toward understanding of self-electrophoretic propulsion under realistic conditions: from bulk reactions to confinement effects. Acc Chem Res. 2018;51(12):2998–3005.
[118] Luo M, Li S, Wan J, Yang C, Chen B, Guan J. Enhanced propulsion of urease-powered micromotors by multilayered assembly of ureases on janus magnetic microparticles. Langmuir. 2020;36(25):7005–13.
[119] Liu M, Yu H, Zhao T, Li X. Emerging enzyme-based nanocomposites for catalytic biomedicine. Dalton Trans. 2023;52(42):15203–15.
[120] Gao S, Liu C, Yang X, Lan Z, Zuo M, Yang P, et al. New synthetic strategy toward a natural enzyme–nanozyme hybrid dual-function nanomotor and its application in environmental remediation. Catal Sci Technol. 2024;14(5):1239–54.
[121] Šípová-Jungová H, Andrén D, Jones S, Käll M. Nanoscale inorganic motors driven by light: principles, realizations, and opportunities. Chem Rev. 2019;120(1):269–87.
[122] Zhou LM, Shi Y, Zhu X, Hu G, Cao G, Hu J, et al. Recent progress on optical micro/nanomanipulations: structured forces, structured particles, and synergetic applications. ACS Nano. 2022;16(9):13264–78.
[123] Rikken RSM, Nolte RJM, Maan JC, van Hest JCM, Wilson DA, Christianen PCM. Manipulation of micro- and nanostructure motion with magnetic fields. Soft Matter. 2014;10(9):1295–308.
[124] Zhou H, Mayorga-Martinez CC, Pané S, Zhang L, Pumera M. Magnetically driven micro and nanorobots. Chem Rev. 2021;121(8):4999–5041.
[125] Wang Q, Yang L, Yu J, Chiu PWY, Zheng Y-P, Zhang L. Real-time magnetic navigation of a rotating colloidal microswarm under ultrasound guidance. IEEE Trans Biomed Eng. 2020;67(12):3403–12.
[126] Xu T, Xu L-P, Zhang X. Ultrasound propulsion of micro-/nanomotors. Appl Mater Today. 2017;9:493–503.
[127] Wang Y, Tu Y, Peng F. The energy conversion behind micro-and nanomotors. Micromachines. 2021;12(2):222.
[128] Garcia-Gradilla V, Orozco J, Sattayasamitsathit S, Soto F, Kuralay F, Pourazary A, et al. Functionalized ultrasound-propelled magnetically guided nanomotors: toward practical biomedical applications. ACS Nano. 2013;7(10):9232–40.

[129] Choi V, Rajora MA, Zheng GJBC. Activating drugs with sound: mechanisms behind sonodynamic therapy and the role of nanomedicine. Bioconjugate Chem. 2020;31:967–89.
[130] Lin X, Song J, Chen X, Yang H. Ultrasound-activated sensitizers and applications. Angew Chem Int Ed. 2020;59(34):14212–33.
[131] Ahmed S, Wang W, Bai L, Gentekos DT, Hoyos M, Mallouk TE. Density and shape effects in the acoustic propulsion of bimetallic nanorod motors. ACS Nano. 2016;10(4):4763–9.
[132] Nadal F, Lauga E. Asymmetric steady streaming as a mechanism for acoustic propulsion of rigid bodies. Phys Fluids. 2014;26(8):041916–1276.
[133] Chen H, Brayman AA, Bailey MR, Matula TJ. Blood vessel rupture by cavitation. Urol Res. 2010;38(4):321–6.
[134] Couture O, Larrat B, Aubry JF, Kassel N, Foley J. Review of ultrasound mediated drug delivery for cancer treatment: updates from pre-clinical studies. Transl Cancer Res. 2014;3(5):494–511.
[135] María Hormigos R, Jurado Sánchez B, Escarpa A. Multi-light-responsive quantum dot sensitized hybrid micromotors with dual-mode propulsion. Angew Chem Int Ed. 2019;58(10):3128–32.
[136] Gao W, Manesh KM, Hua J, Sattayasamitsathit S, Wang J. Hybrid nanomotor: a catalytically/magnetically powered adaptive nanowire swimmer. Small. 2011;7(14):2047–51.
[137] Afsari T, Nowlin K, Weissing C, Ahmed S. Nanorobotic system with fine control over multiple modes of motion. ACS Appl Nano Mater. 2023;7:18435–42.
[138] Wu Z, Wu R, Li X, Wang X, Tang X, Tan K, et al. Multi-pathway microenvironment regulation for atherosclerosis therapy based on beta-cyclodextrin/l-arginine/au nanomotors with dual-mode propulsion. Small. 2021;18(9):2104120.
[139] Wang H, Chen X, Qi Y, Wang C, Huang L, Wang R, et al. Self-fueled janus nanomotors as active drug carriers for propulsion behavior-reinforced permeability and accumulation at the tumor site. Chem Mater. 2022;34(16):7543–52.
[140] Zheng Z, Zheng X, Kong D, Ding K, Zhang Z, Zhong R, et al. Pressure-gradient counterwork of dual-fuel driven nanocarriers in abnormal interstitial fluids for enhancing drug delivery efficiency. Small. 2023;19(24):2207252.
[141] Chen L, Fang D, Zhang J, Xiao X, Li N, Li Y, et al. Nanomotors-loaded microneedle patches for the treatment of bacterial biofilm-related infections of wound. J Colloid Interface Sci. 2023;647:142–51.
[142] Roussos ET, Condeelis JS, Patsialou A. Chemotaxis in cancer. Nat Rev Cancer. 2011;11(8):573–87.
[143] Ji Y, Lin X, Wu Z, Wu Y, Gao W, He Q. Macroscale chemotaxis from a swarm of bacteria-mimicking nanoswimmers. Angew Chem Int Ed. 2019;58(35):12200–5.
[144] Baraban L, Harazim SM, Sanchez S, Schmidt OG. Chemotactic behavior of catalytic motors in microfluidic channels. Angew Chem. 2013;52(21):5552–6.
[145] Wang X, Ye Z, Lin S, Wei L, Xiao L. Nanozyme-triggered cascade reactions from cup-shaped nanomotors promote active cellular targeting. Research. 2022;2022:9831012.
[146] Yang Y, Zhao YJL. Discretized motion of surface walker under a nonuniform AC magnetic field. Langmuir. 2020;36(37):11125–37.
[147] Vyas SP, Singh A, Sihorkar V. Ligand-receptor-mediated drug delivery: an emerging paradigm in cellular drug targeting. Crit Rev Ther Drug Carrier Syst. 2001;18(1):1–76.
[148] Fang D, Li T, Wu Z, Wang Q, Wan M, Zhou M, et al. Dual drive mode polydopamine nanomotors for continuous treatment of an inferior vena cava thrombus. J Mater Chem B. 2021;9(41):8659–66.
[149] Wan MM, Chen H, Da Wang Z, Liu ZY, Yu YQ, Li L, et al. Nitric oxide-driven nanomotor for deep tissue penetration and multidrug resistance reversal in cancer therapy. Adv Sci. 2020;8(3):2002525.
[150] Lu Y, Liu S, Liang J, Wang Z, Hou Y. Self-propelled nanomotor for cancer precision combination therapy. Adv Healthc Mater. 2024;13:e2304212.
[151] Xuan M, Shao J, Gao C, Wang W, Dai L, He Q. Self-propelled nanomotors for thermomechanically percolating cell membranes. Angew Chem Int Ed. 2018;57(38):12463–7.
[152] Ou J, Liu K, Jiang J, Wilson DA, Liu L, Wang F, et al. Micro-/nanomotors toward biomedical applications: the recent progress in biocompatibility. Small. 2020;16(27):1906184.
[153] Tian H, Ou J, Wang Y, Sun J, Gao J, Ye Y, et al. Bladder microenvironment actuated proteomotors with ammonia amplification for enhanced cancer treatment. Acta Pharm Sin B. 2023;13(9):3862–75.
[154] Zhou M, Xing Y, Li X, Du X, Xu T, Zhang X. Cancer cell membrane camouflaged semi-yolk@spiky-shell nanomotor for enhanced cell adhesion and synergistic therapy. Small. 2020;16(39):2003834.
[155] Liu A, Wang Q, Zhao Z, Wu R, Wang M, Li J, et al. Nitric oxide nanomotor driving exosomes-loaded microneedles for achilles tendinopathy healing. ACS Nano. 2021;15:13339–50.
[156] Zhao S, Duan F, Liu S, Wu T, Shang Y, Tian R, et al. Efficient intracellular delivery of RNase A using DNA origami carriers. ACS Appl Mater Interfaces. 2019;11(12):11112–8.
[157] Tejeda-Rodríguez JA, Núñez A, Soto F, García-Gradilla V, Cadena-Nava R, Wang J, et al. Virus-based nanomotors for cargo delivery. ChemNanoMat. 2018;5(2):194–200.
[158] Magdanz V, Sanchez S, Schmidt OG. Development of a sperm-flagella driven micro-bio-robot. Adv Mater. 2013;25(45):6581–8.
[159] Wu Z, Li T, Li J, Gao W, Xu T, Christianson C, et al. Turning erythrocytes into functional micromotors. ACS Nano. 2014;8(12):12041–8.
[160] Stanton MM, Simmchen J, Ma X, Miguel-López A, Sánchez S. Biohybrid janus motors driven by Escherichia coli. Adv Mater Interfaces. 2015;3(2):1500505.
[161] Stanton MM, Park BW, Miguel-López A, Ma X, Sitti M, Sánchez S. Biohybrid microtube swimmers driven by single captured bacteria. Small. 2017;13(19):1603679.
[162] Mathuriya AS. Magnetotactic bacteria for cancer therapy. Biotechnol Lett. 2014;37(3):491–8.
[163] Shi YZ, Xiong S, Zhang Y, Chin LK, Chen Y, Zhang JB, et al. Sculpting nanoparticle dynamics for single-bacteria-level screening and direct binding-efficiency measurement. Nat Commun. 2018;9(1):815.
[164] Zhou M, Xing Y, Li X, Du X, Xu T, Zhang X, et al. Cancer cell membrane camouflaged semi-yolk@spiky-shell nanomotor for enhanced cell adhesion and synergistic therapy. Small. 2020;16(39):2003834.
[165] Zeng M, Huang D, Wang P, King D, Peng B, Luo J, et al. Autonomous catalytic nanomotors based on 2D magnetic nanoplates. ACS Appl Nano Mater. 2019;2(3):1267–73.
[166] Wu B, Fu J, Zhou Y, Luo S, Zhao Y, Quan G, et al. Tailored core–shell dual metal–organic frameworks as a versatile nanomotor for effective synergistic antitumor therapy. Acta Pharm Sin B. 2020;10(11):2198–211.
[167] Amouzadeh Tabrizi M, Shamsipur M, Saber R, Sarkar S. Isolation of HL-60 cancer cells from the human serum sample using MnO_2-PEI/Ni/Au/aptamer as a novel nanomotor and electrochemical

determination of thereof by aptamer/gold nanoparticles-poly (3,4-ethylene dioxythiophene) modified GC electrode. Biosens Bioelectron. 2018;110:141–6.
[168] Hansen-Bruhn M, de Ávila BE, Beltrán-Gastélum M, Zhao J, Ramírez-Herrera DE, Angsantikul P, et al. Active Intracellular delivery of a Cas9/sgRNA complex using ultrasound-propelled nanomotors. Angew Chem Int Ed. 2018;57(10):2657–61.
[169] Sun J, Mathesh M, Li W, Wilson DA. Enzyme-powered nanomotors with controlled size for biomedical applications. ACS Nano. 2019;13(9):10191–200.
[170] Tu Y, Peng F, Heuvelmans JM, Liu S, Nolte RJM, Wilson DA. Motion Control of polymeric nanomotors based on host–guest interactions. Angew Chem Int Ed. 2019;58(26):8687–91.
[171] Lu X, Ou H, Wei Y, Ding X, Wang X, Zhao C, et al. Superfast fuel-free tubular hydrophobic micromotors powered by ultrasound. Sens Actuators B. 2022;372:372.
[172] Maric T, Løvind A, Zhang Z, Geng J, Boisen A. Near-infrared light-driven mesoporous SiO_2/Au nanomotors for eradication of pseudomonas aeruginosa biofilm. Adv Healthc Mater. 2023;12(13):2203018.
[173] Gao W, Dong R, Thamphiwatana S, Li J, Gao W, Zhang L, et al. Artificial micromotors in the mouse's stomach: a step toward in vivo use of synthetic motors. ACS Nano. 2015;9(1):117–23.
[174] Peng F, Men Y, Tu Y, Chen Y, Wilson DA. Nanomotor-based strategy for enhanced penetration across vasculature model. Adv Funct Mater. 2018;28(25):1706117.
[175] O'Brien JS. Cell membranes–composition: structure: function. J Theor Biol. 1967;15(3):307–24.
[176] de Visser KE, Joyce JA. The evolving tumor microenvironment: From cancer initiation to metastatic outgrowth. Cancer Cell. 2023;41(3):374–403.
[177] Song Y, Zhan G, Zhou SF. Design of near infrared light-powered copper phyllosilicate nanomotors for cuproptosis-based synergistic cancer therapy. Adv Funct Mater. 2024;34(18):2314568.
[178] Qualliotine JR, Bolat G, Beltrán-Gastélum M, de Ávila BEF, Wang J, Califano JA. Acoustic nanomotors for detection of human papillomavirus–associated head and neck cancer. Otolaryngol–Head Neck Surg. 2019;161(5):814–22.
[179] Wu Z, Li L, Yang Y, Hu P, Gao W. A microrobotic system guided by photoacoustic computed tomography for targeted navigation in intestines *in vivo*. Sci Robot. 2019;4(32):eaax0613.
[180] Ge Y, Li Y, Bai Y, Yuan C, Wu C, Hu Y. Visible light-driven multi-motion modes CNC/TiO2 nanomotors for highly efficient degradation of emerging contaminants. Carbon. 2019;155:195–203.
[181] Oroojalian F, Beygi M, Baradaran B, Mokhtarzadeh A, Shahbazi MA. Immune cell membrane-coated biomimetic nanoparticles for targeted cancer therapy. Small. 2021;17(12):e2006484.
[182] Tezel G, Timur SS, Kuralay F, Gürsoy RN, Ulubayram K, Öner L, et al. Current status of micro/nanomotors in drug delivery. J Drug Target. 2021;29(1):29–45.
[183] Lee EJ, Guenther CM, Suh J. Adeno-associated virus (AAV) vectors: Rational design strategies for capsid engineering. Curr Opin Biomed Eng. 2018;7:58–63.
[184] Li Z, Wang Y, Liu J, Rawding P, Bu J, Hong S, et al. Chemically and biologically engineered bacteria-based delivery systems for emerging diagnosis and advanced therapy. Adv Mater. 2021;33(38):e2102580.
[185] Nikezić AV, Novaković JG. Nano/microcarriers in drug delivery: moving the timeline to contemporary. Curr Med Chem. 2023;30(26):2996–3023.
[186] Yoshizumi Y, Suzuki H. Self-propelled metal–polymer hybrid micromachines with bending and rotational motions. ACS Appl Mater Interfaces. 2017;9:21355–61.
[187] Han K, Shields CW, Diwakar NM, Bharti B, López GP, Velev OD. Sequence-encoded colloidal origami and microbot assemblies from patchy magnetic cubes. Sci Adv. 2017;3(8):e1701108.
[188] Chen Z, Xia T, Zhang Z, Xie S, Li X. Enzyme-powered Janus nanomotors launched from intratumoral depots to address drug delivery barriers. Chem Eng J. 2019;375:122109.
[189] Wang M, Zhang S, Song Y, Dong J, Wei H, Xie H, et al. 3D printed microtransporters: compound micromachines for spatiotemporally controlled delivery of therapeutic agents. Nanotechnology. 2016;27(42):6644–50.
[190] McNeill JM, Nitesh N, Braxton JM, Mallouk TE. Wafer-scale fabrication of micro- to nanoscale bubble swimmers and their fast autonomous propulsion by ultrasound. J ACS Nano. 2020;14(6):7520–8.
[191] Mark AG, Gibbs JG, Lee TC, Fischer P. Hybrid nanocolloids with programmed three-dimensional shape and material composition. Nat Mat. 2013;12(9):802–7.
[192] Gibbs JG, Zhao Y. Self-organized multiconstituent catalytic nanomotors. Small. 2010;6(15):1656–62.
[193] Xu B, Lei H, Tong T, Guan Y, Wang Y, Li B, et al. Acidity-actuated polymer/calcium phosphate hybrid nanomotor (PCaPmotor) for penetrating drug delivery and synergistic anticancer immunotherapy. Nano Lett. 2024;24(35):10724–33.
[194] Lin X, Dong X, Sun Y. Dual-carbon dots composite: a multifunctional photo-propelled nanomotor against alzheimer's β-Amyloid. Small. 2024;20:e2407154.
[195] Bai X, Peng W, Tang Y, Wang Z, Guo J, Song F, et al. An NIR-propelled janus nanomotor with enhanced ROS-scavenging, immunomodulating and biofilm-eradicating capacity for periodontitis treatment. Bioact Mater. 2024;41:271–92.